Recent Results on Heavy Quark Production in High Energy Nucleus-Nucleus Collisions

Xin Dong

Lawrence Berkeley National Laboratory

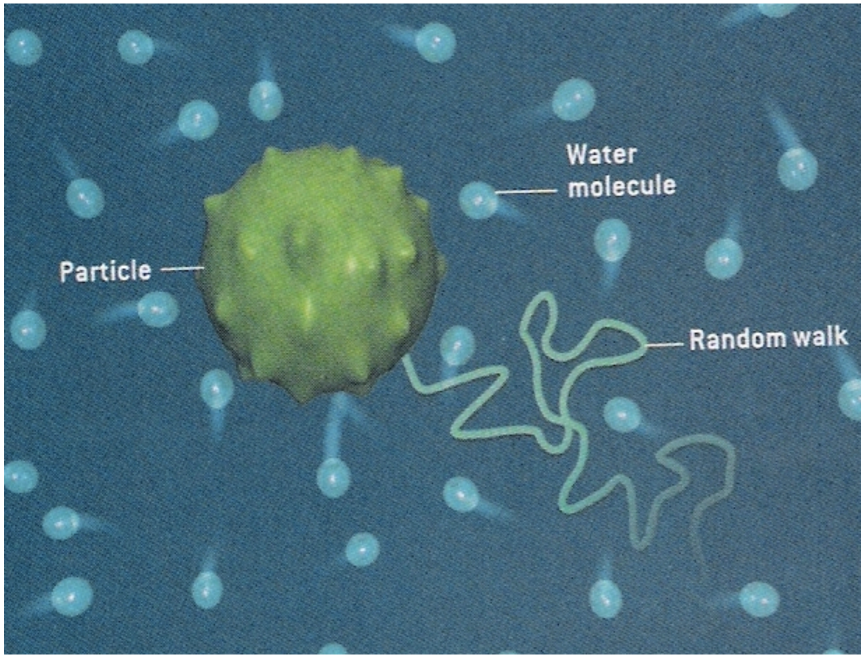

~ 10-100 nm

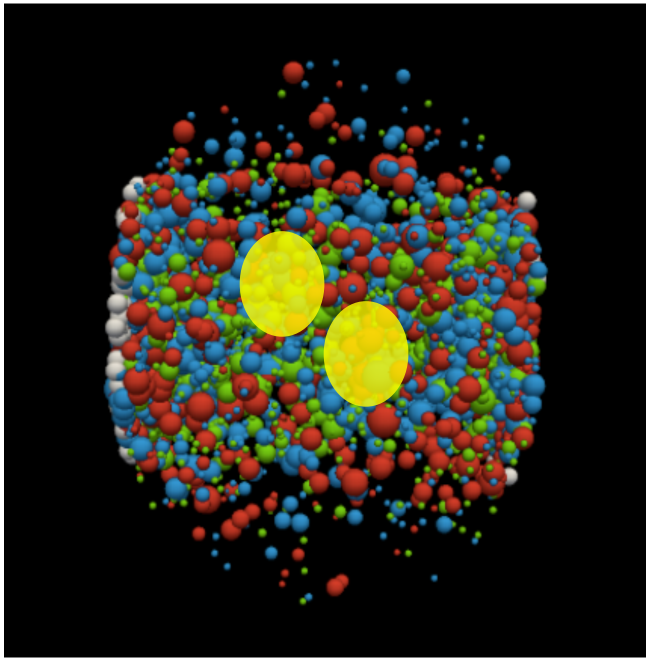

~10 fm

Quark-Gluon Plasma and Early Universe

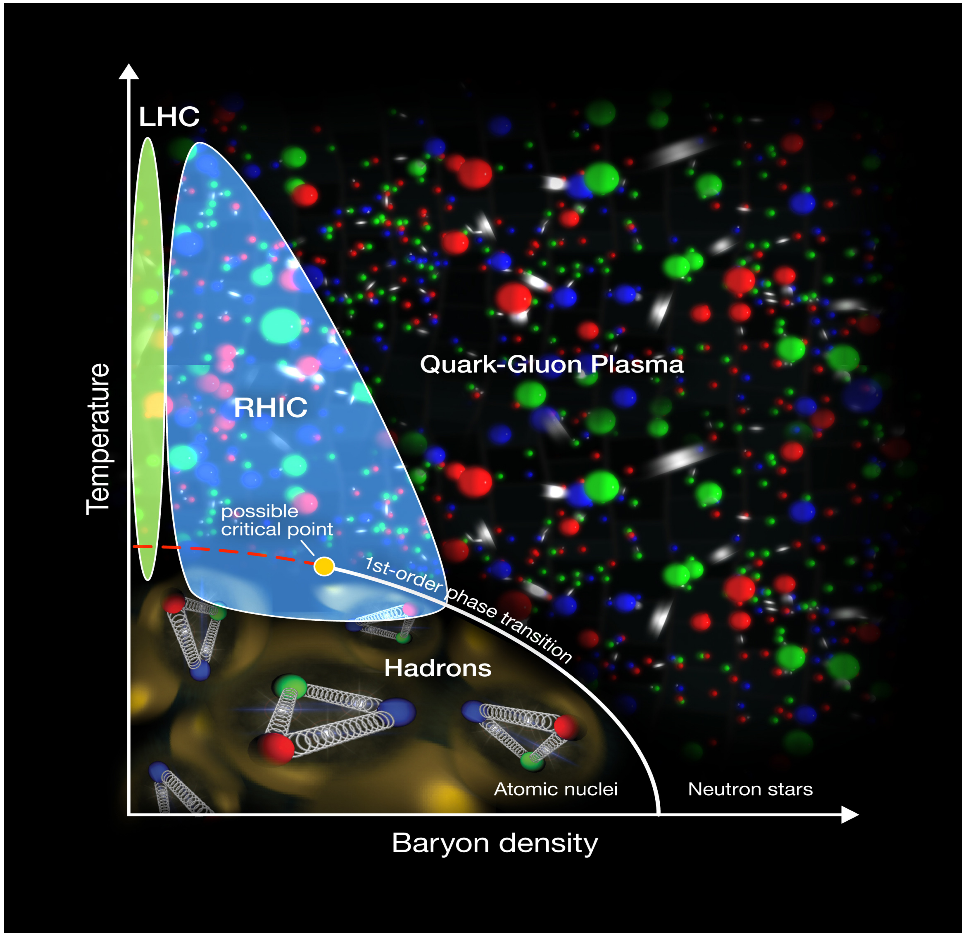

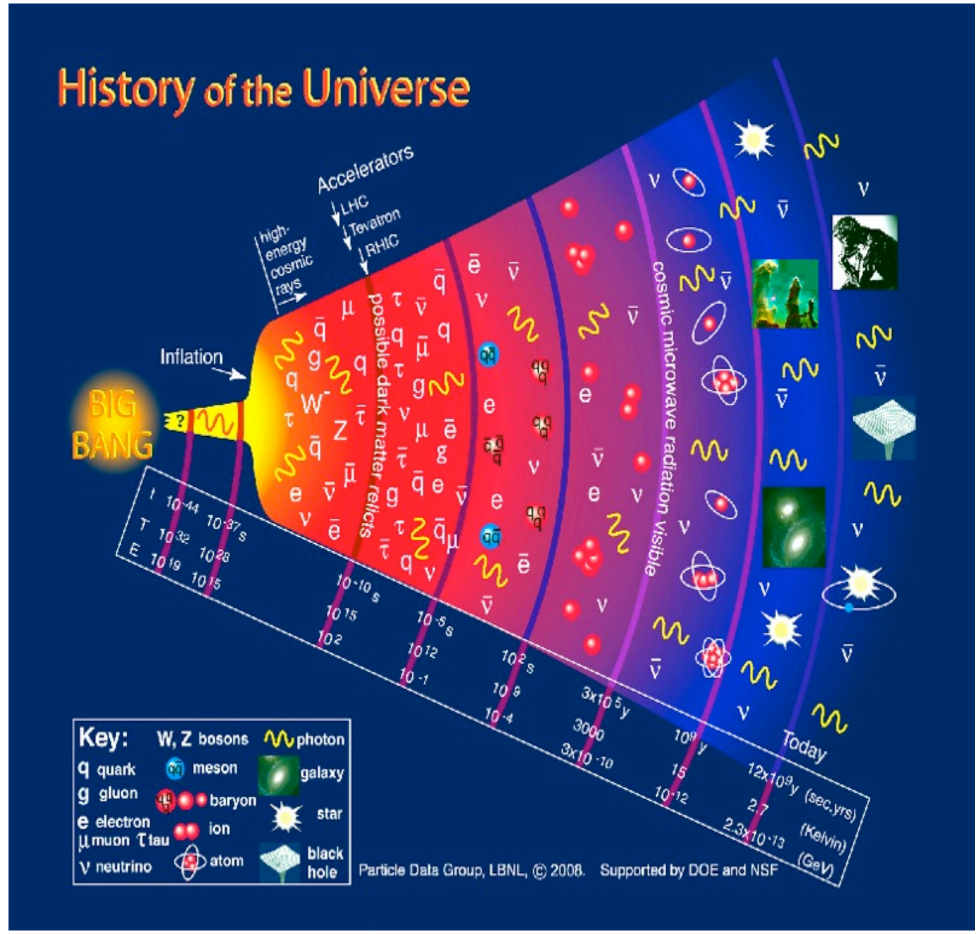

- Lattice QCD predicts a new state of QCD matter at high temperature/density
  - quark-gluon plasma (quarks and gluons not confined within hadrons)
- Expected to be the state of early universe a few μs after Big-Bang

High Energy Nucleus-Nucleus Collisions

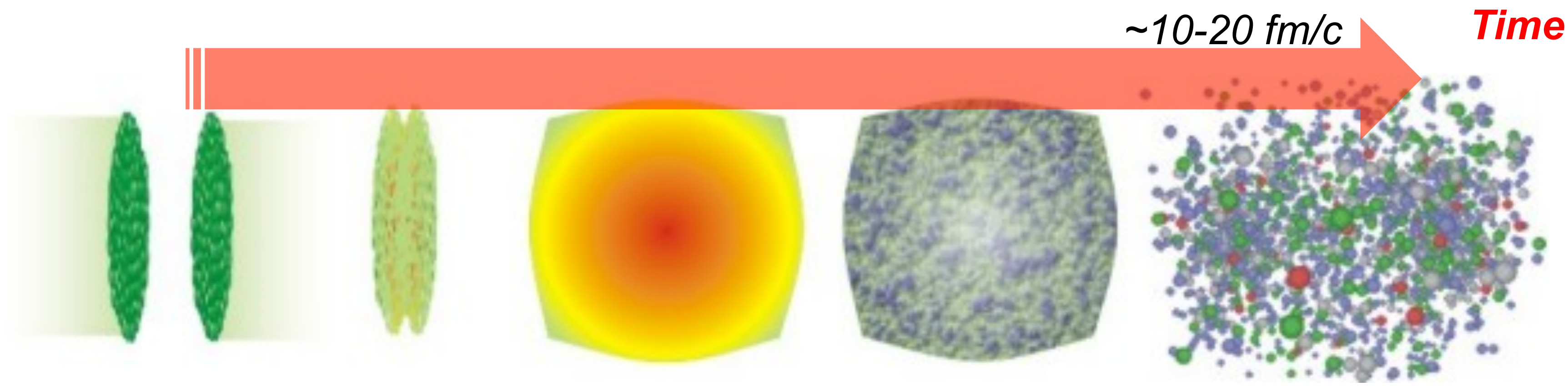

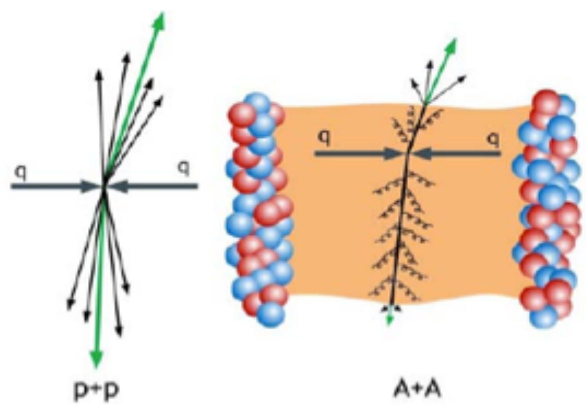

Nuclear modification factor (R_{AA})

$$R_{AA} = \frac{d^2N^{AA}/dp_T dy}{N_{bin} d^2N^{pp}/dp_T dy}$$

Characterize the medium effect

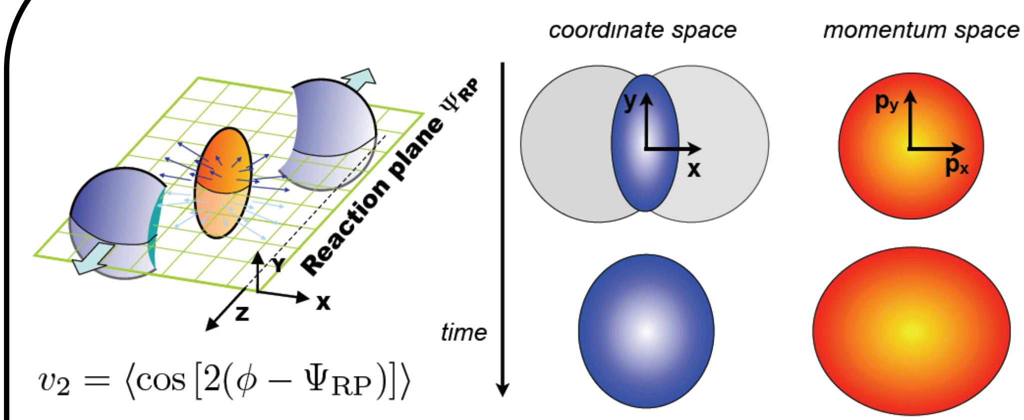

$$v_2 = \langle \cos[2(\phi - \Psi_{RP})] \rangle$$

Elliptic flow (v_2) = 2nd Fourier coefficient

Sensitive to the early stage properties

RHIC Discoveries

"Jet Quenching"

- Significant suppression in particle yield at high p_T in central heavy ion collisions

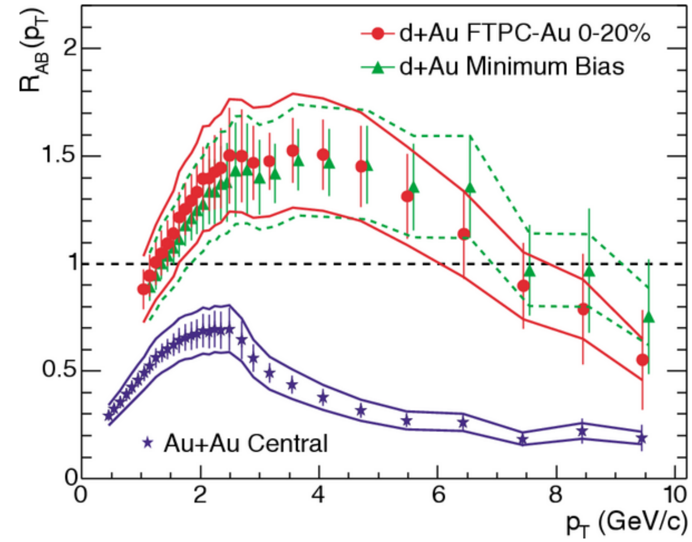

STAR: PRL. 91 (2003) 072304

"Partonic Collectivity"

- Strong collective flow, even for multi-strange hadrons (ϕ, Ω)
- Flow driven by Number-of-Constituent-Quark (NCQ) in hadrons

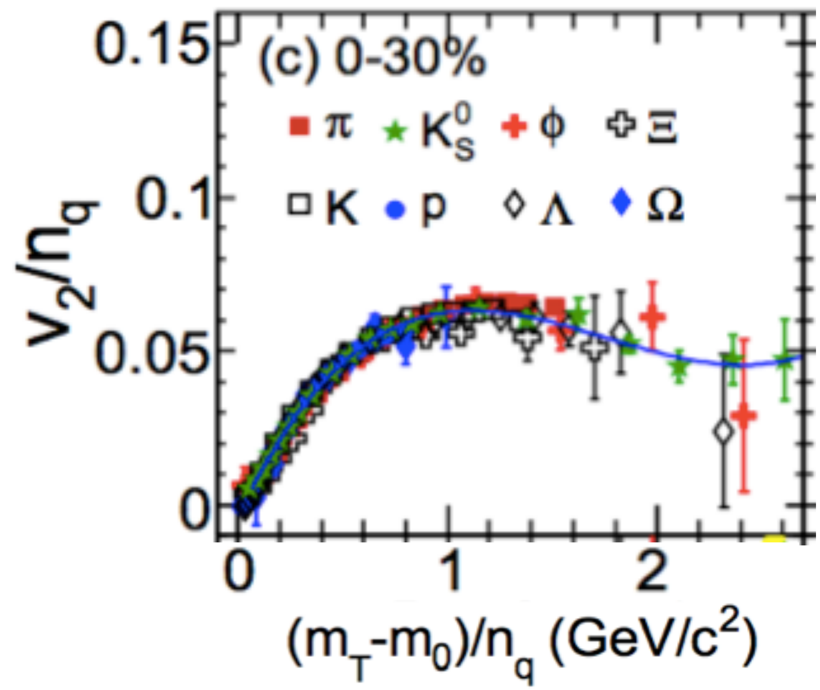

STAR: PRL. 99 (2007) 112301

Formation of strongly-coupled Quark Gluon Plasma (sQGP)!

- Re-affirmed by LHC measurements

Quantitative Measure of QGP

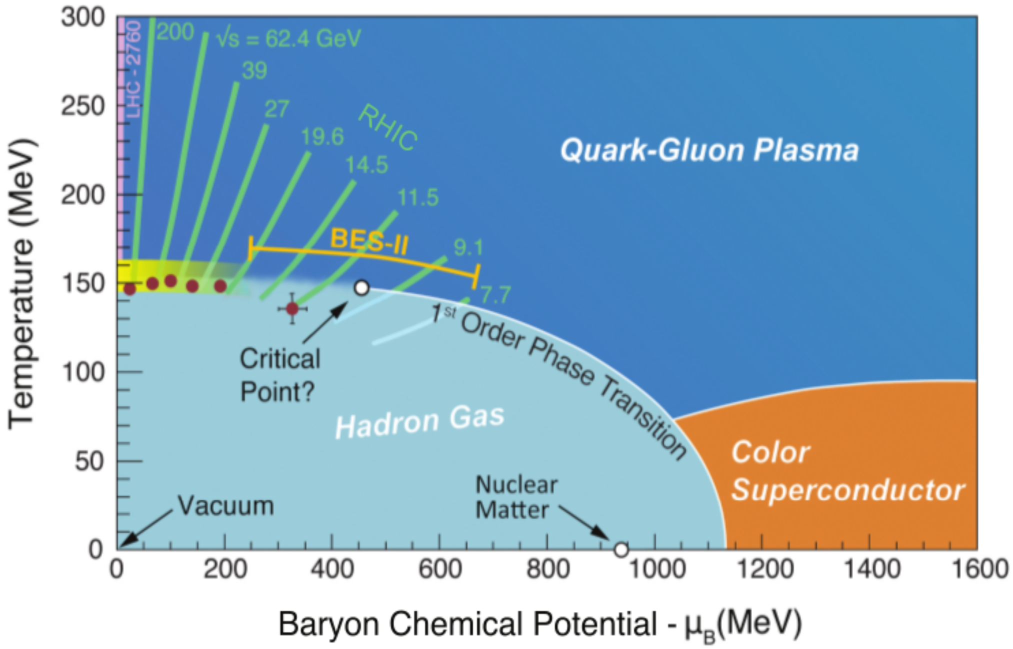

At top RHIC and LHC energies:

To precisely determine (temperature dependence of) **emergent** QCD transport parameters in QGP

- ***η/s*** - *gluons*
- ***q-hat*** - *high energy partons*
- ***D_s*** - *heavy quarks*
- …

JET Coll., PRC 90 (2015) 014909
Hot QCD white paper - arXiv: 1502.02730

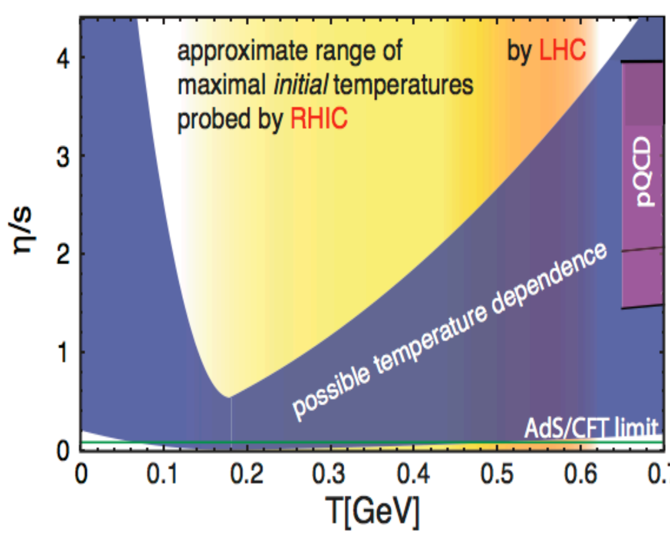

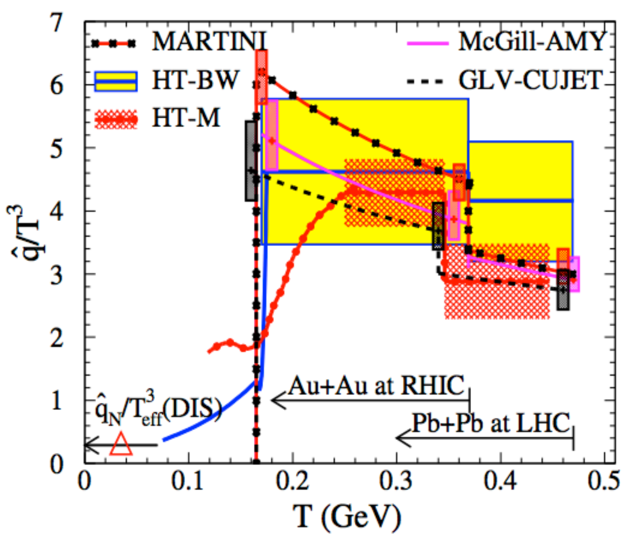

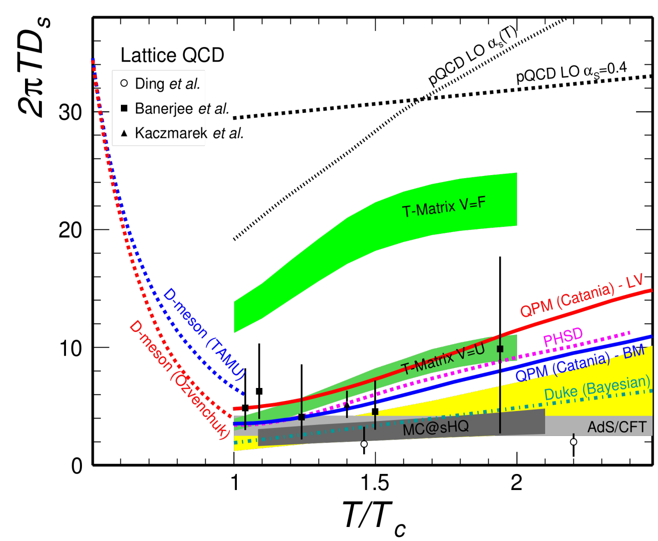

Uniqueness of Heavy Quarks in QCD

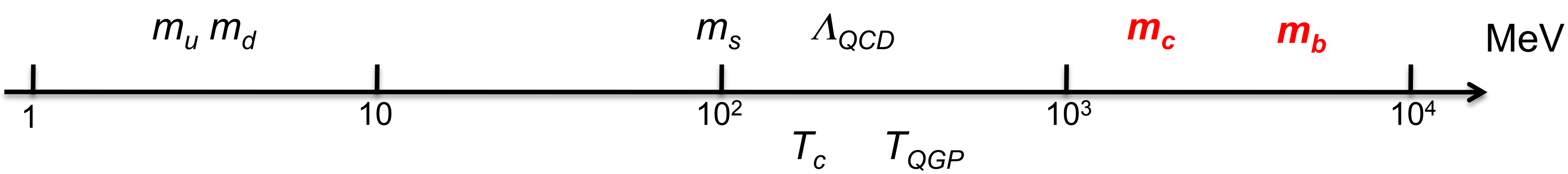

$m_{c,b} >> \Lambda_{QCD}$ *amenable to perturbative QCD*

$m_{c,b} >> T_{QGP}$ *predominately created from initial hard scatterings*

Collisional energy loss

Radiative energy loss

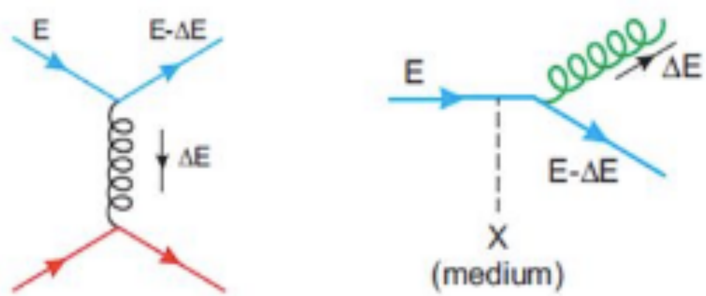

Heavy quarks

- sensitive to

different energy loss mechanisms

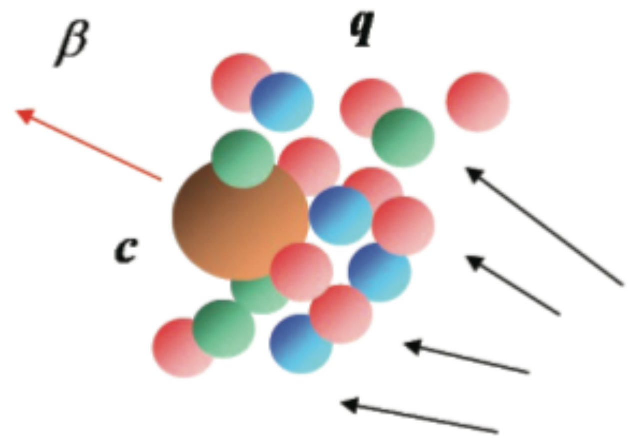

When $M_{HQ} >> T$, $M_{HQ} >> gT$

"Brownian" motion → Langevin simu. $\frac{dp^i}{dt} = -\eta_D p^i + \xi^i(t)$,

drag

fluctuations

Diffusion coefficient D_s

Brownian Motion and Einstein's Theory

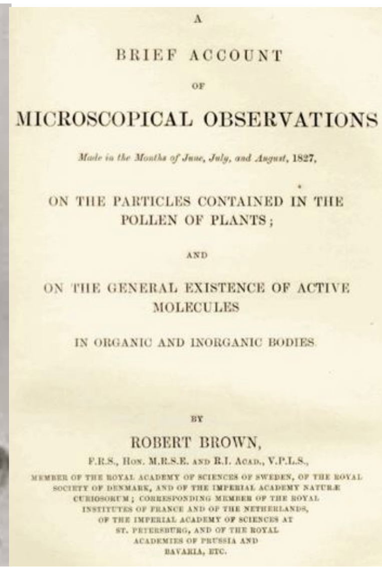

A

BRIEF ACCOUNT

OF

MICROSCOPICAL OBSERVATIONS

Made in the Months of June, July, and August, 1827,

ON THE PARTICLES CONTAINED IN THE POLLEN OF PLANTS;

AND

ON THE GENERAL EXISTENCE OF ACTIVE MOLECULES

IN ORGANIC AND INORGANIC BODIES

BY

ROBERT BROWN,

F.R.S., HON. M.R.S.E. AND R.I. ACAD., V.P.L.S.,

MEMBER OF THE ROYAL ACADEMY OF SCIENCES OF SWEDEN, OF THE ROYAL SOCIETY OF DENMARK, AND OF THE IMPERIAL ACADEMY NATURÆ CURIOSORUM; CORRESPONDING MEMBER OF THE ROYAL INSTITUTES OF FRANCE AND OF THE NETHERLANDS, OF THE IMPERIAL ACADEMY OF SCIENCES AT ST. PETERSBURG, AND OF THE ROYAL ACADEMIES OF PRUSSIA AND BAVARIA, ETC.

Robert Brown, 1827

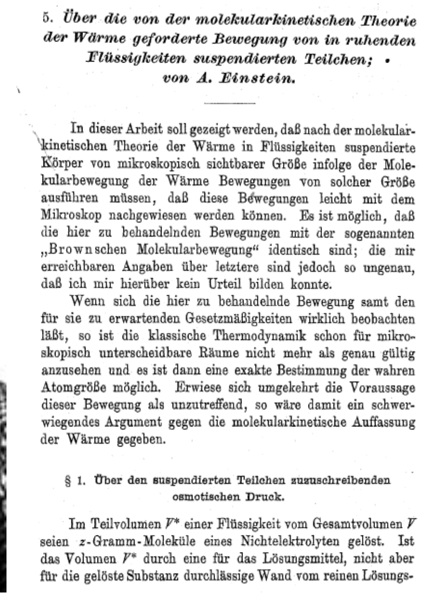

5. ***Über die von der molekularkinetischen Theorie der Wärme geforderte Bewegung von in ruhenden Flüssigkeiten suspendierten Teilchen; von A. Einstein.***

In dieser Arbeit soll gezeigt werden, daß nach der molekularkinetischen Theorie der Wärme in Flüssigkeiten suspendierte Körper von mikroskopisch sichtbarer Größe infolge der Molekularbewegung der Wärme Bewegungen von solcher Größe ausführen müssen, daß diese Bewegungen leicht mit dem Mikroskop nachgewiesen werden können. Es ist möglich, daß die hier zu behandelnden Bewegungen mit der sogenannten „Brownschen Molekularbewegung" identisch sind; die mir erreichbaren Angaben über letztere sind jedoch so ungenau, daß ich mir hierüber kein Urteil bilden konnte.

Wenn sich die hier zu behandelnde Bewegung samt den für sie zu erwartenden Gesetzmäßigkeiten wirklich beobachten läßt, so ist die klassische Thermodynamik schon für mikroskopisch unterscheidbare Räume nicht mehr als genau gültig anzusehen und es ist dann eine exakte Bestimmung der wahren Atomgröße möglich. Erwiese sich umgekehrt die Voraussage dieser Bewegung als unzutreffend, so wäre damit ein schwerwiegendes Argument gegen die molekularkinetische Auffassung der Wärme gegeben.

§ 1. Über den suspendierten Teilchen zuzuschreibenden osmotischen Druck.

Im Teilvolumen V^* einer Flüssigkeit vom Gesamtvolumen V seien z-Gramm-Moleküle eines Nichtelektrolyten gelöst. Ist das Volumen V^* durch eine für das Lösungsmittel, nicht aber für die gelöste Substanz durchlässige Wand vom reinen Lösungs-

Albert Einstein, 1905

- Brownian Motion – jittery motion of pollen grains in water
- Einstein's 1905 paper mathematically explained the Brownian motion

$$\frac{\partial \rho}{\partial t} = D \frac{\partial^2 \rho}{\partial x^2} \qquad \langle x^2(t) \rangle - \langle x^2(0) \rangle \sim Dt$$

D – diffusion coefficient

- Validated by Jean Perrin's experiment in 1909 (awarded Nobel Prize in 1926)

Physics Goals of Heavy Quark Measurements in HIC

- Mass dependence of parton energy loss - $\Delta E_g > \Delta E_q > \Delta E_c > \Delta E_b$
- Quantify QGP transport parameter - HQ spatial diffusion coefficient, $\boldsymbol{D_s}$

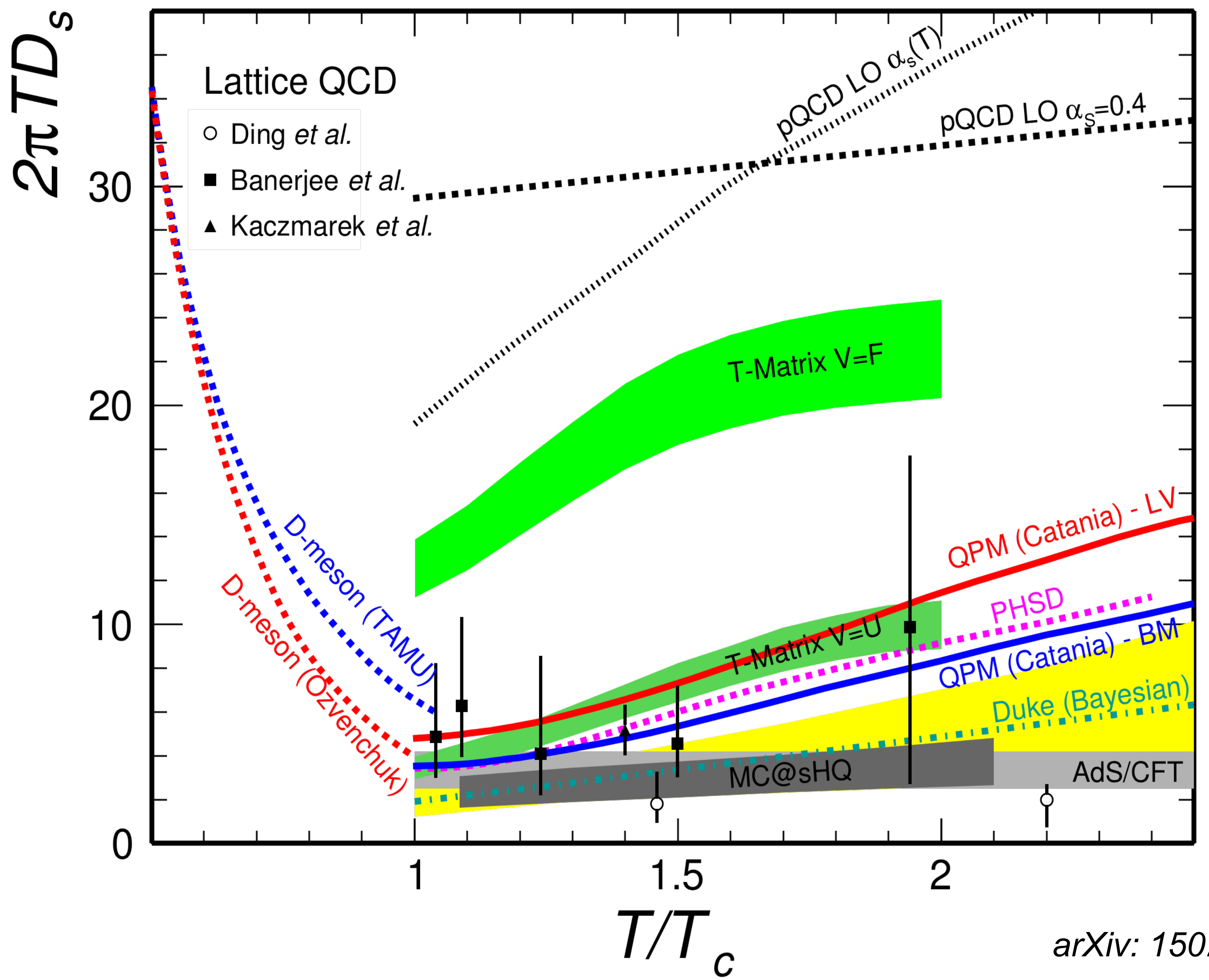

arXiv: 1502.02730

Experimental Methods

Hadron	Abundance (fragmentation)	cτ (μm)
D^0	56%	123
D^+	24%	312
D_s	10%	150
Λ_c	10%	60
B^+	40%	491
B^0	40%	456

1) Secondary vertex reconstruction
   e.g. $D^0 \to K\pi$, $B \to J/\psi K$

2) Inclusive impact parameter method
   e.g. $D/B \to e$, $B \to D$, $B \to J/\psi$ …

Precision silicon vertex tracker is crucial, particularly in high multiplicity heavy-ion collisions

Courtesy of K. Oh

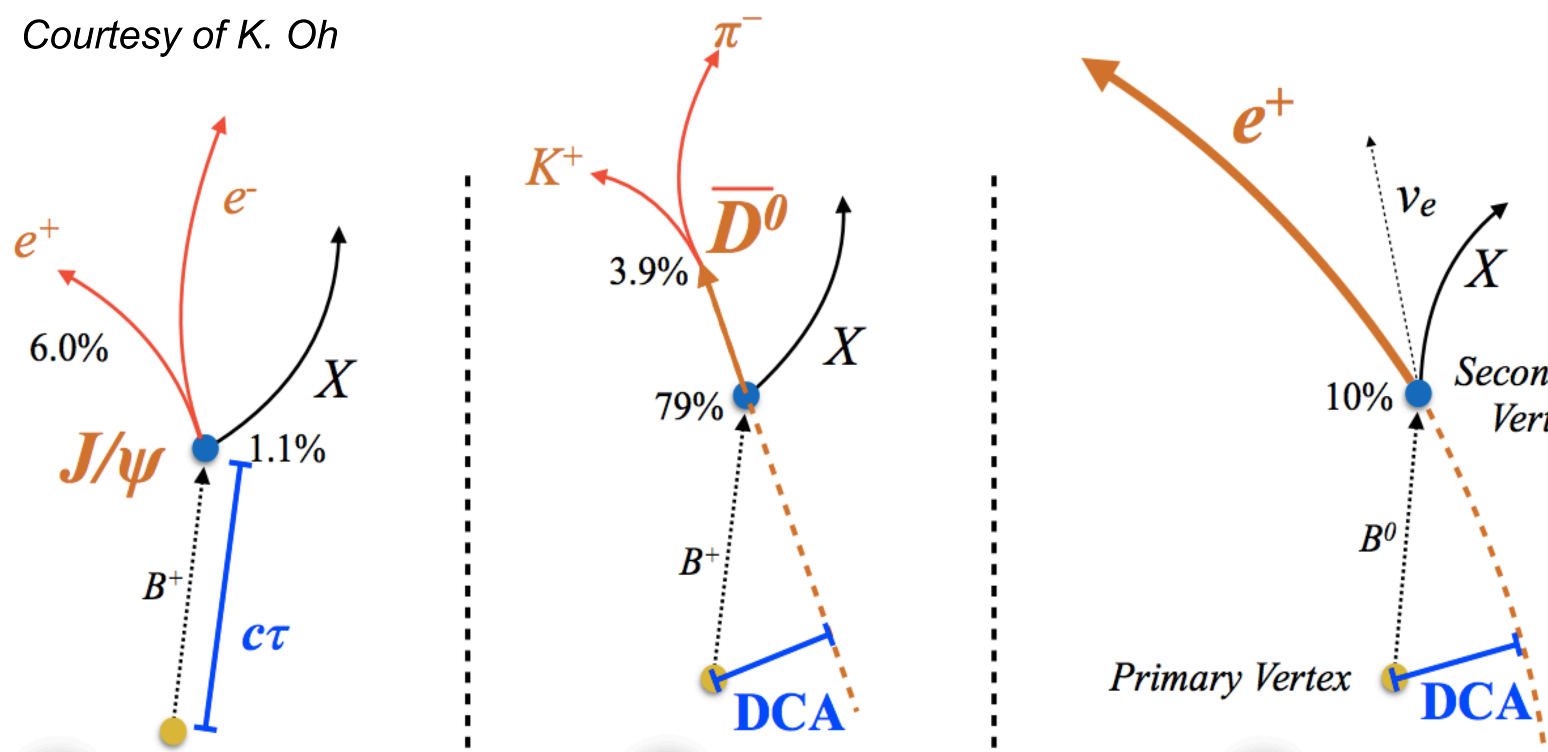

Key Instruments – Pixel Silicon Detector

	ALICE	ATLAS	CMS	LHCb	PHENIX	STAR
Sensor tech.	Hybrid	Hybrid	Hybrid	Hybrid	Hybrid	**MAPS**
Pitch size (μm^2)	50x425	50x400	100x150	200x200	50x425	**20x20**
Radius of first layer (cm)	3.9	5.1	4.4	N/A	2.5	2.8
Thickness of first layer	1%X_0	~1%X_0	~1%X_0	~1%X_0	1%X_0	**0.4%X_0**

STAR Pixel – first application of **MAPS** technology in collider experiments

(MAPS - Monolithic Active Pixel Sensor)

Next generation MAPS planed for future experiments:

ALICE ITS upgrade, sPHENIX MVTX

- to address the QGP medium properties

Also for CBM, EIC detector R&D

Monolithic Active Pixel Sensors (MAPS)

MAPS pixel cross-section (not to scale)

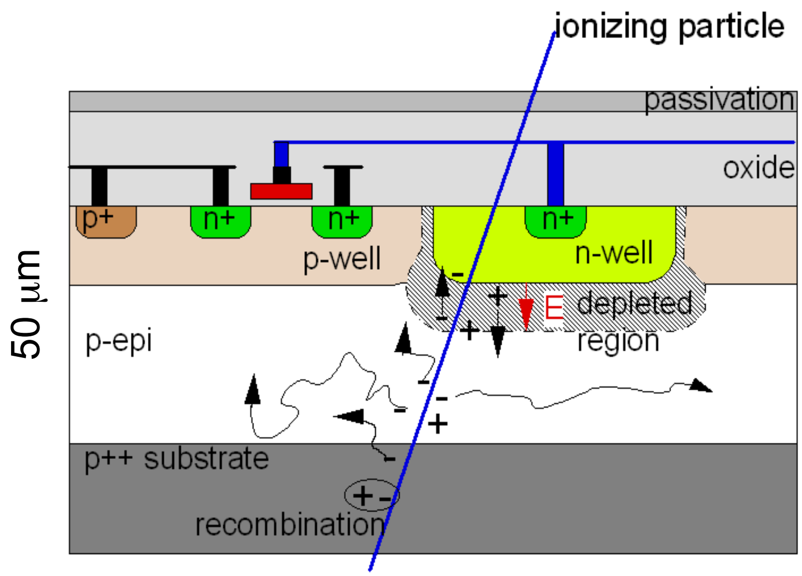

Properties:

- Standard commercial CMOS technology
- Sensor and signal processing are integrated in the same silicon wafer
- Signal is created in the low-doped epitaxial layer (typically ~10-15 µm) → MIP signal is limited to <1000 electrons
- Charge collection is mainly through thermal diffusion (~100 ns), reflective boundaries at p-well and substrate

MAPS and competition	MAPS	Hybrid Pixel	CCD
Granularity	+	-	+
Small material budget	+	-	+
Readout speed	+	++	-
Radiation tolerance	+	++	-

MAPS - particularly chosen for measuring HF hadron decays in heavy ion collisions

A Heavy-Ion Event Display

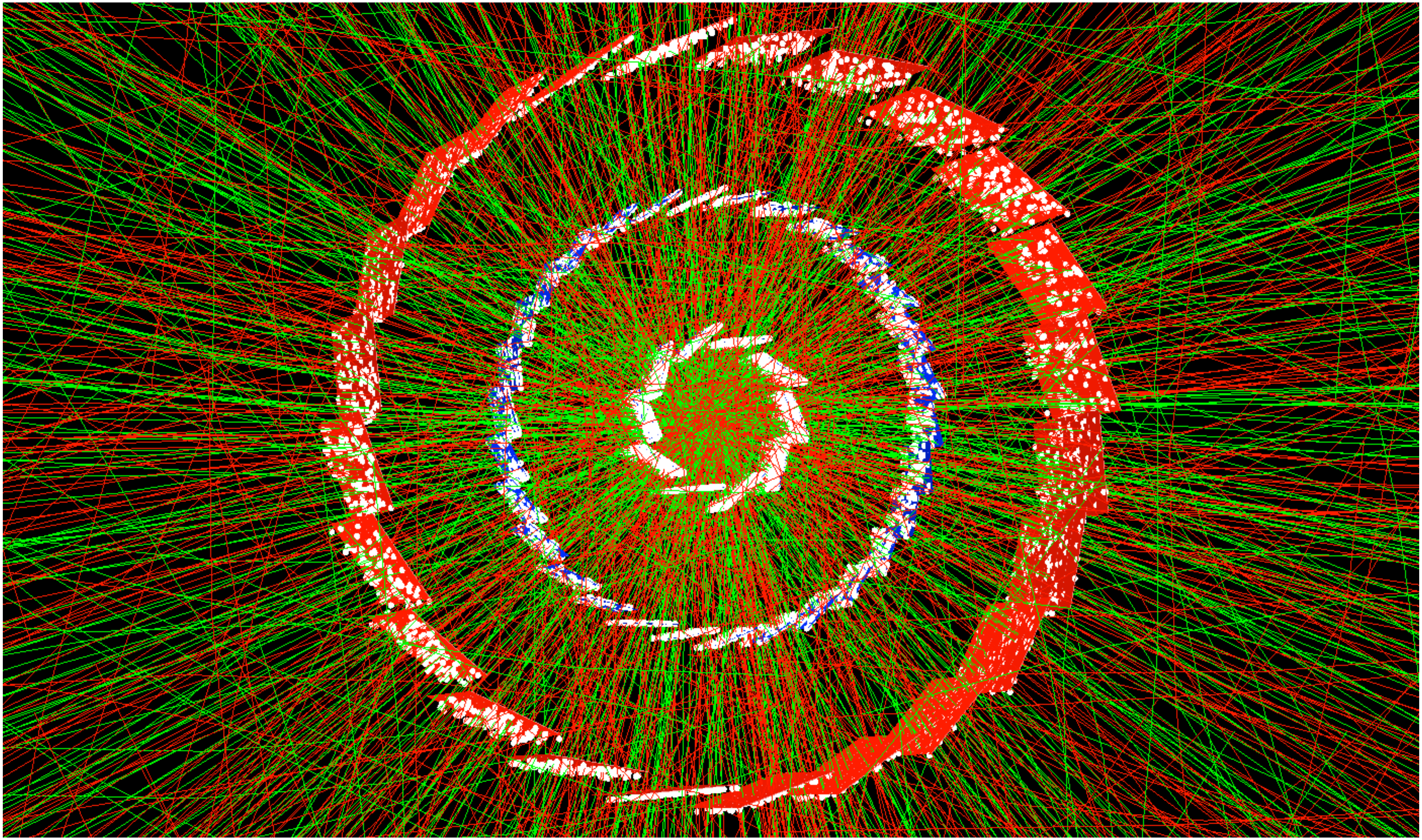

STAR Heavy Flavor Tracker

10 cm

Pixel Detector Performance

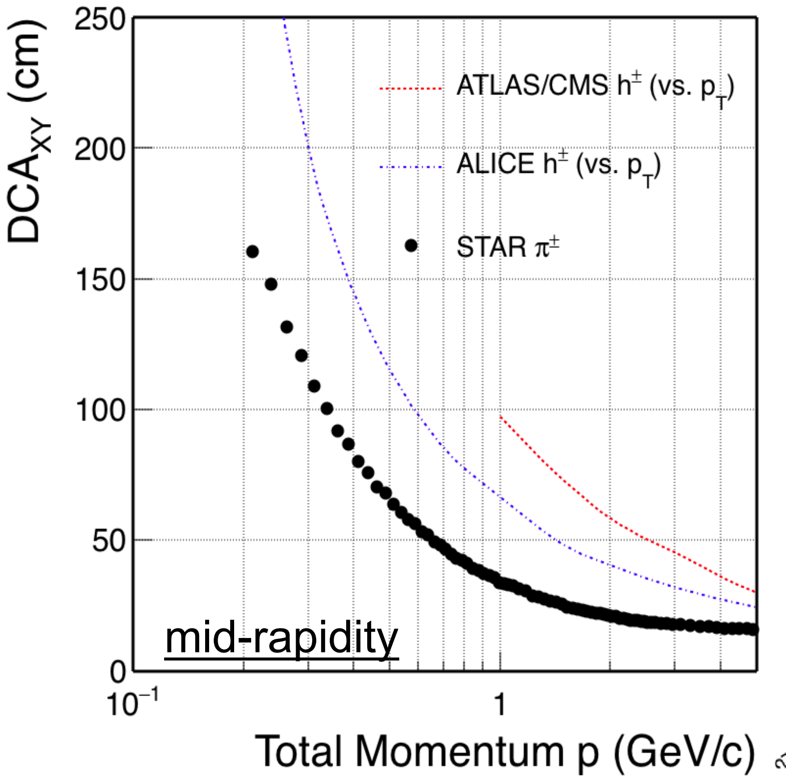

Exclusive reconstruction of HF hadrons
in heavy-ion collisions

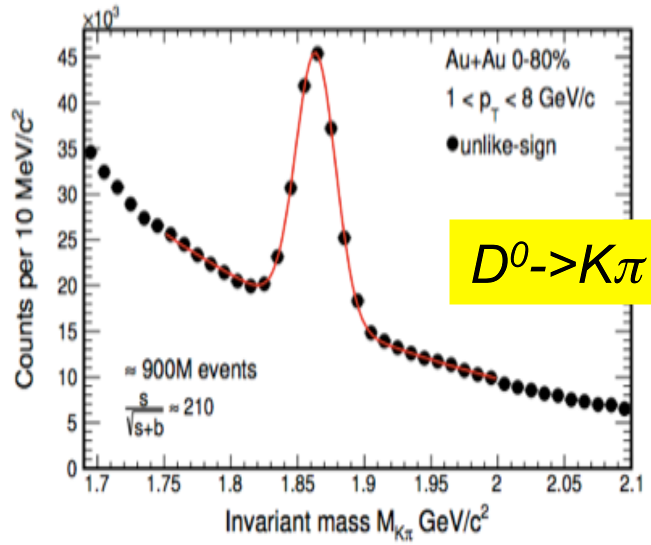

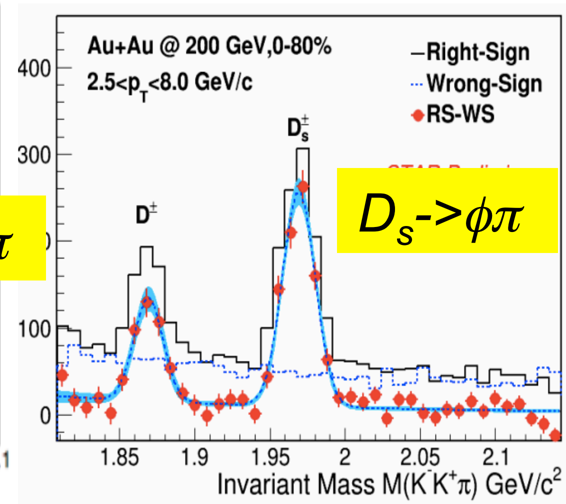

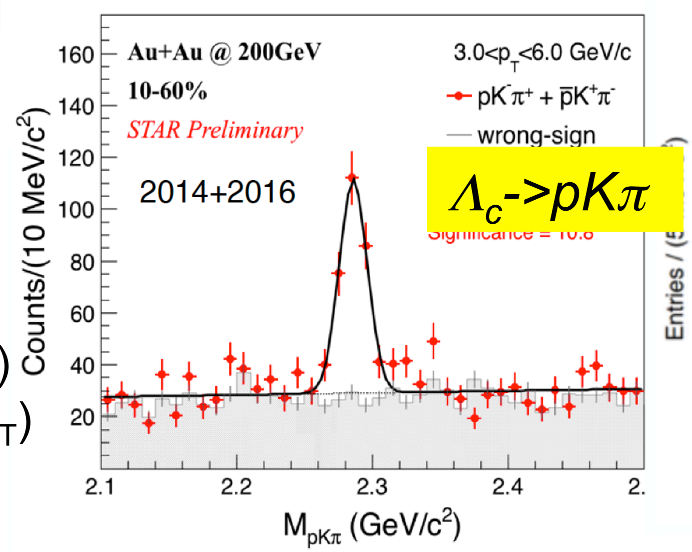

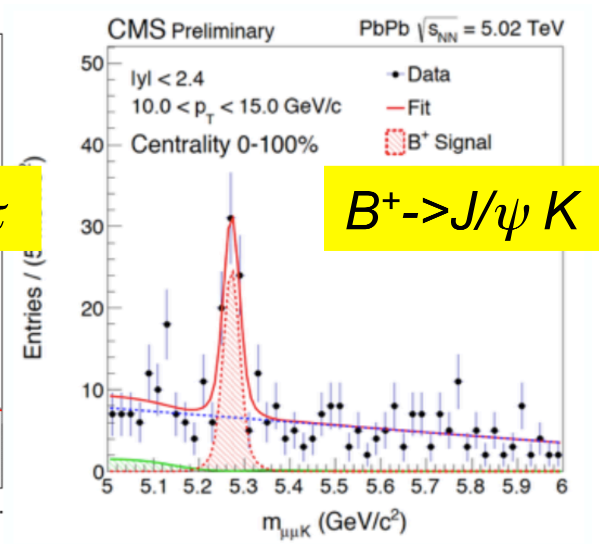

STAR	30 μm @ 1 GeV/c (p)
ALICE	70 μm @ 1 GeV/c (p_T)
ATLAS/CMS	100 μm @ 1 GeV/c (p_T)

Charm Production in p+p Collisions

0.2-7 TeV
mid-rapidity

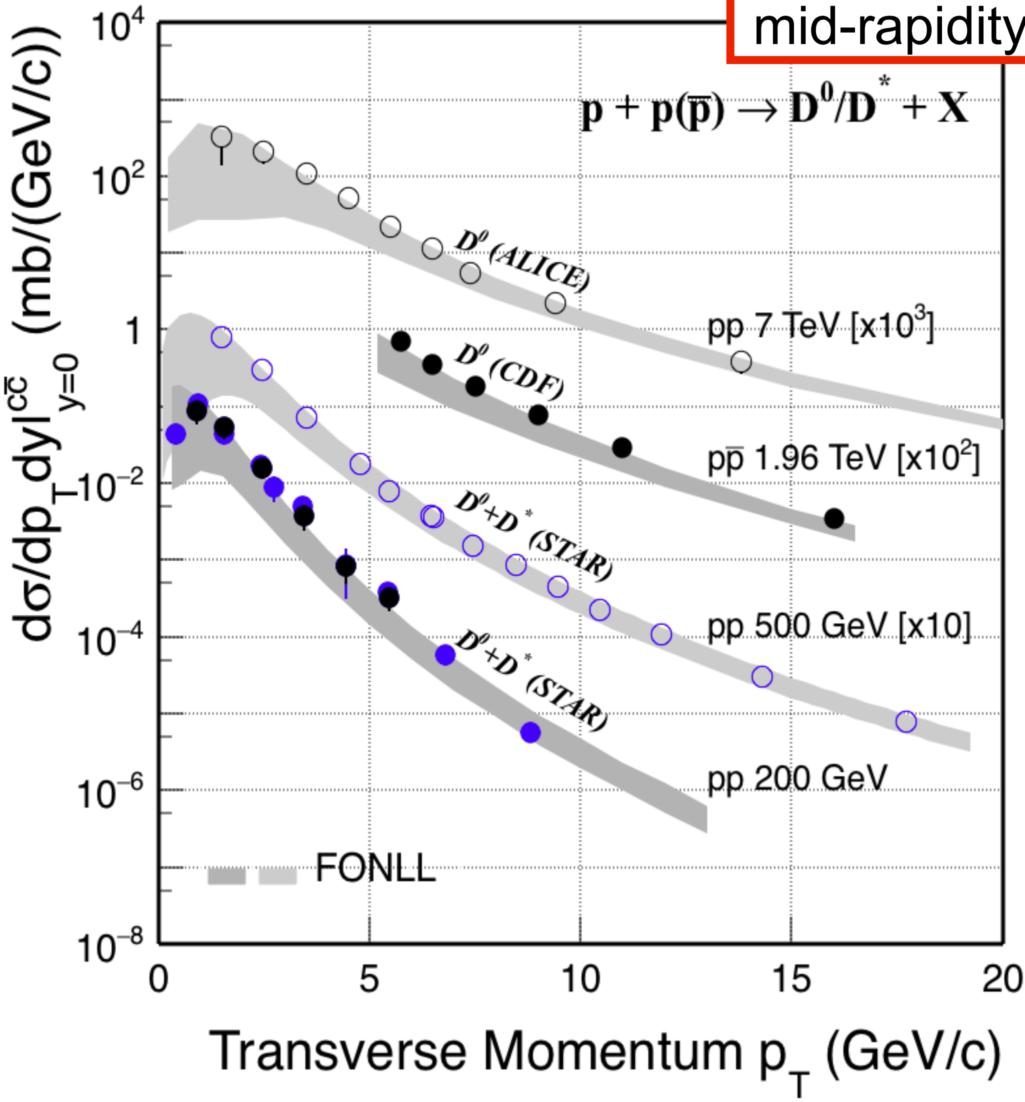

13 TeV
forward-rapidity

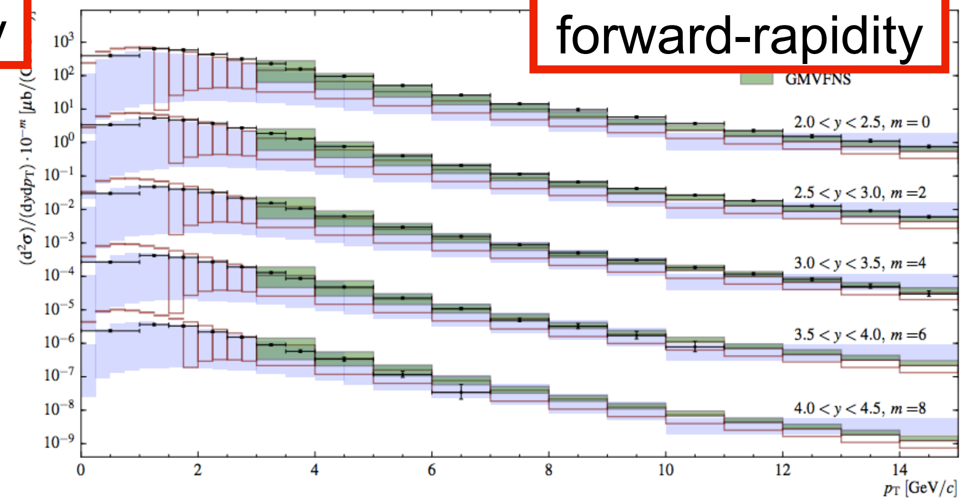

STAR, PRD 86 (2012) 072013, QM14
CDF, PRL 91 (2003) 241804
ALICE, JHEP 01(2012) 128, arXiv: 1702.00766
LHCb, JHEP 03 (2016) 159, 09 (2016) 013

- Charm hadron spectra well described by pQCD FONLL
  - data prefer upper bounds of FONLL calculations

p+A to Constrain Cold Nuclear Matter Effects

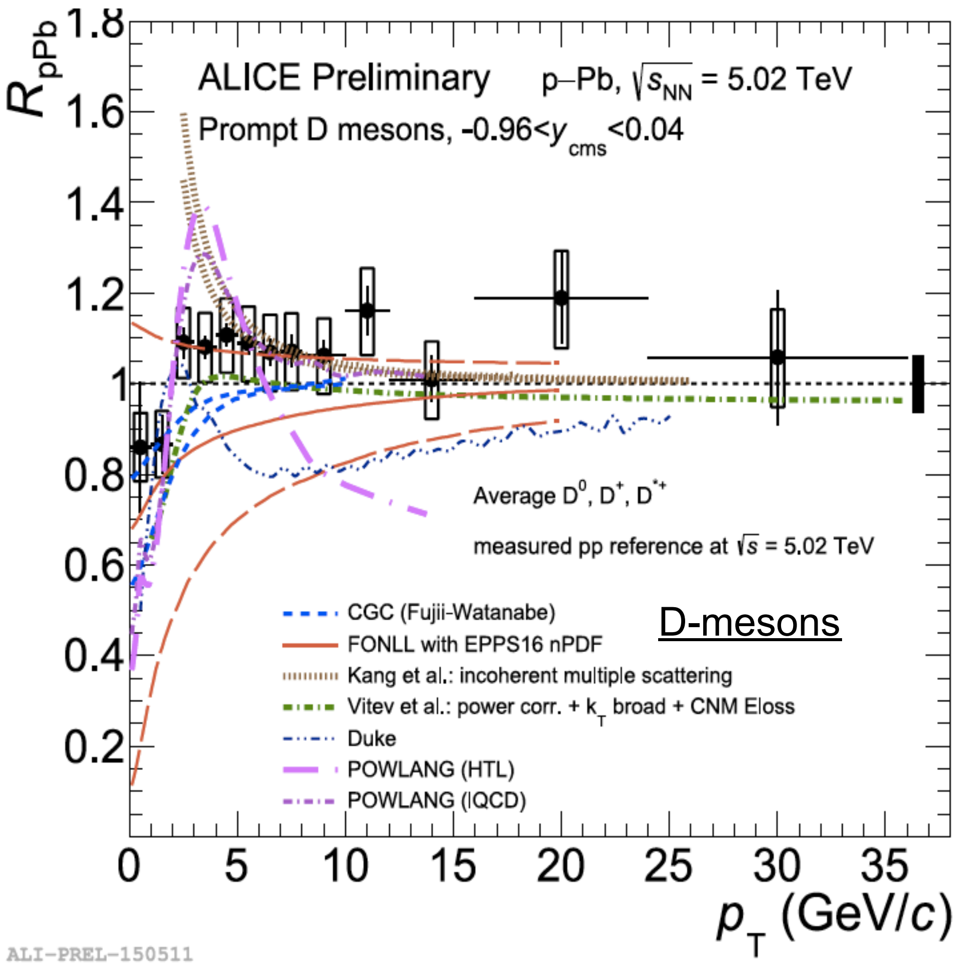

$$R_{\rm FB}(p_{\rm T}, y^*) \equiv \frac{{\rm d}^2\sigma_{p{\rm Pb}}(p_{\rm T}, +|y^*|)/{\rm d}p_{\rm T}{\rm d}y^*}{{\rm d}^2\sigma_{{\rm Pb}p}(p_{\rm T}, -|y^*|)/{\rm d}p_{\rm T}{\rm d}y^*},$$

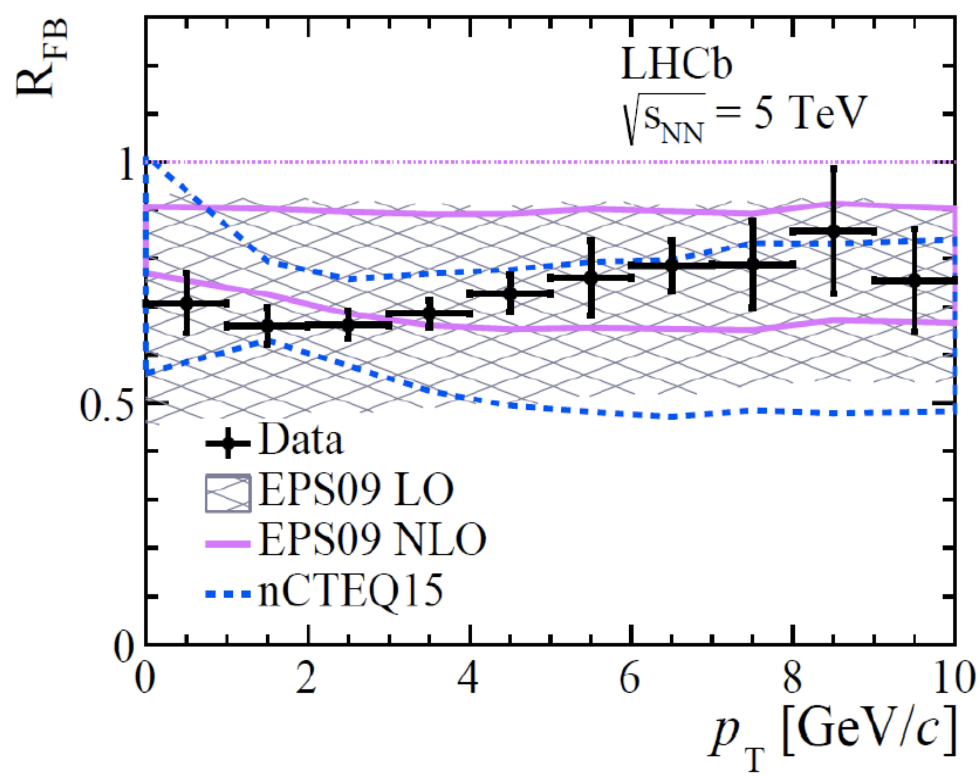

ALICE, PRC 94 (2016) 054908, QM18; LHCb, JHEP 10 (2017) 090

pQCD+nPDF / models with CNM effects describe R_{pPb} at mid-rapidity and F/B asymmetry reasonably well.

Charm Hadron R_{AA} – Energy Loss in Hot QGP

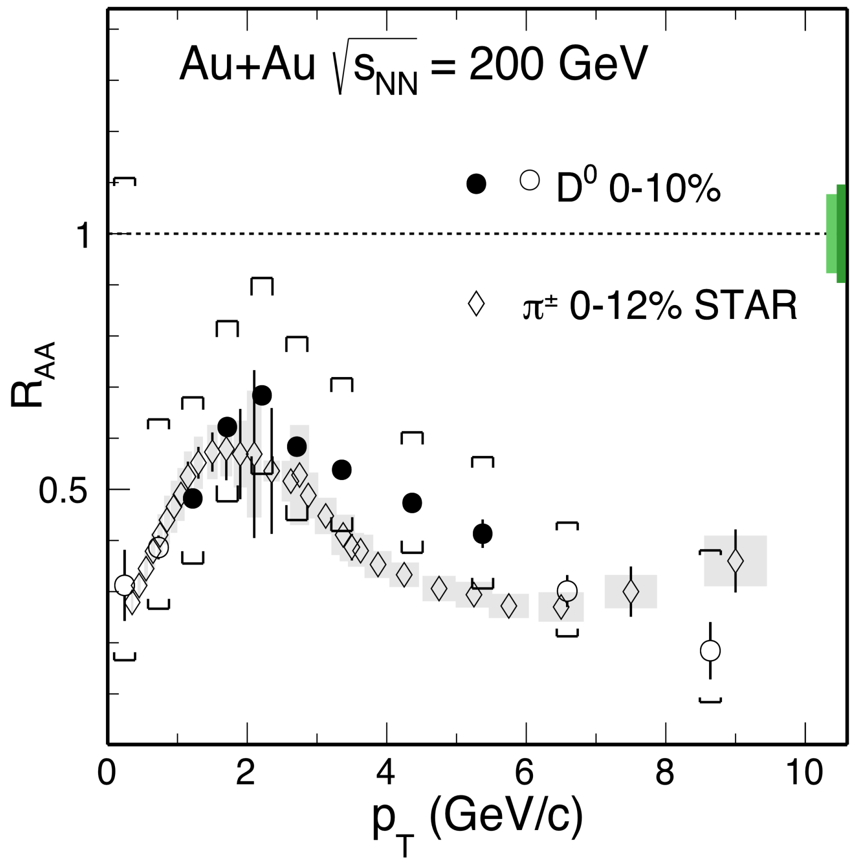

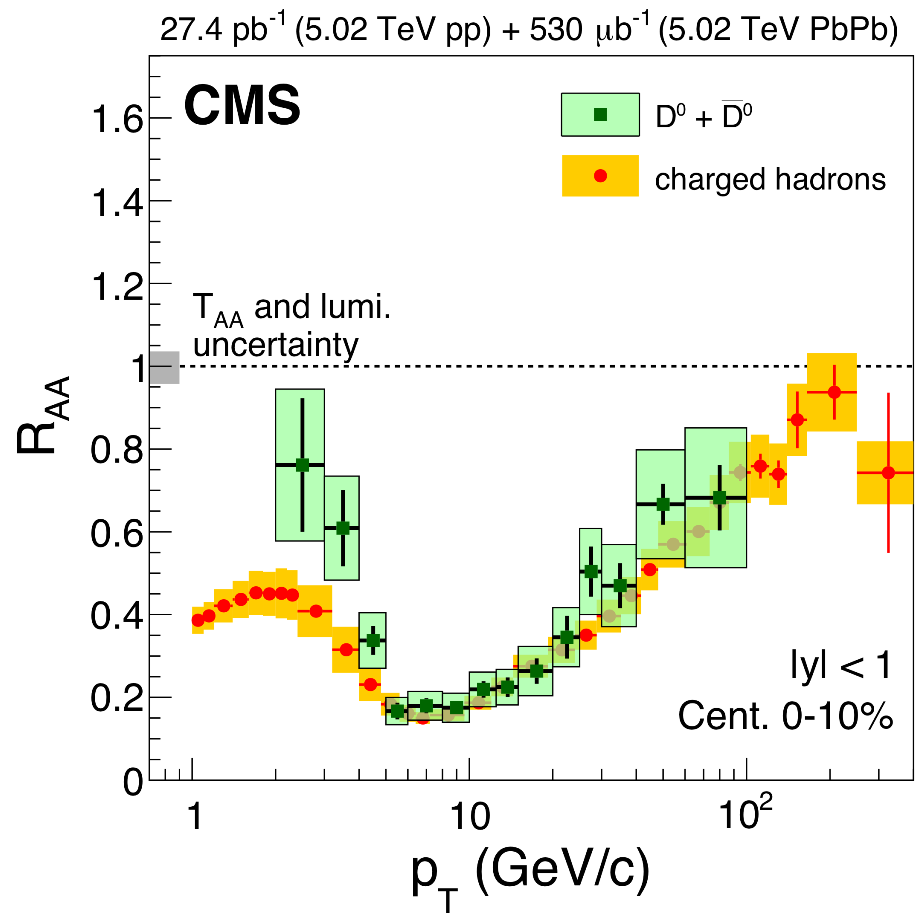

STAR PRL 113 (2014) 142301, QM18; CMS-HIN-16-001

- R_{AA} (D) ~ R_{AA}(h) at p_T > 5 GeV/c in central A+A collisions
  - strong interactions between charm and medium

Charm Hadron v_2 at RHIC

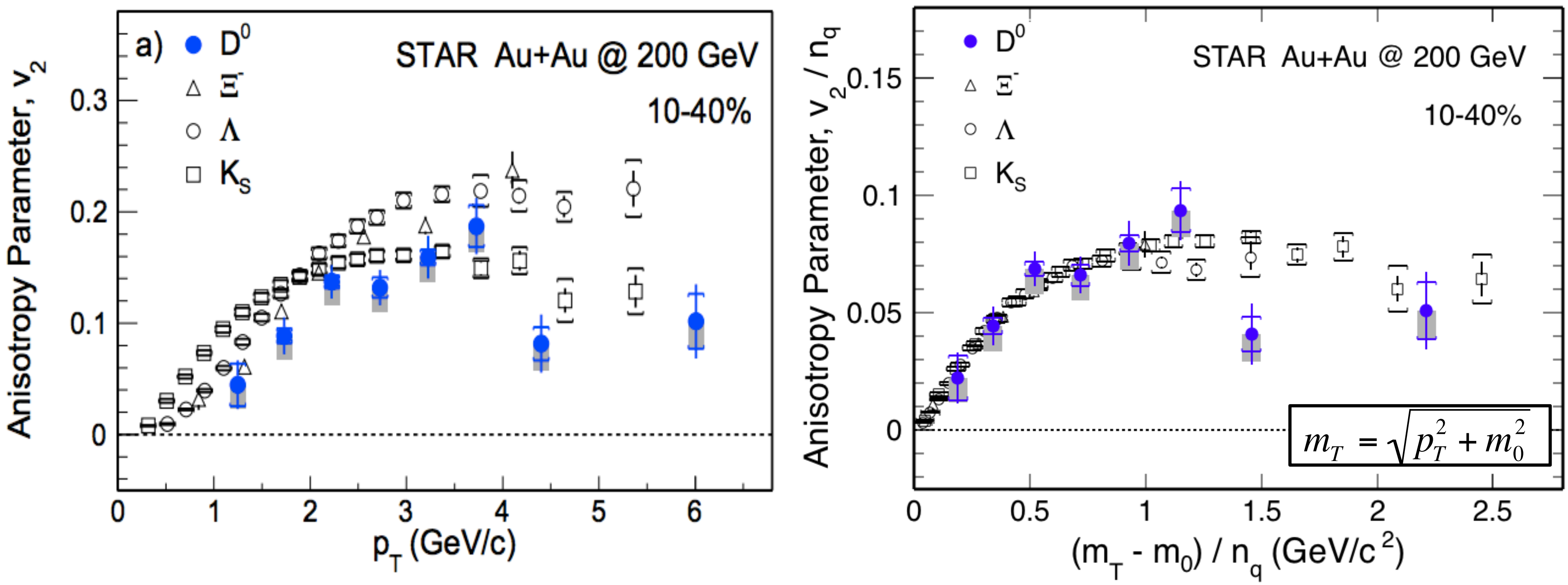

STAR, PRL 118 (2017) 212301

- Mass ordering at p_T < 2 GeV/c (hydrodynamic behavior)
- v_2(D) follows the (m_T-m_0) NCQ scaling as light hadrons below 1 GeV/c^2

Evidence of charm quarks flowing the same with the medium

Charm Hadron v_2 at LHC

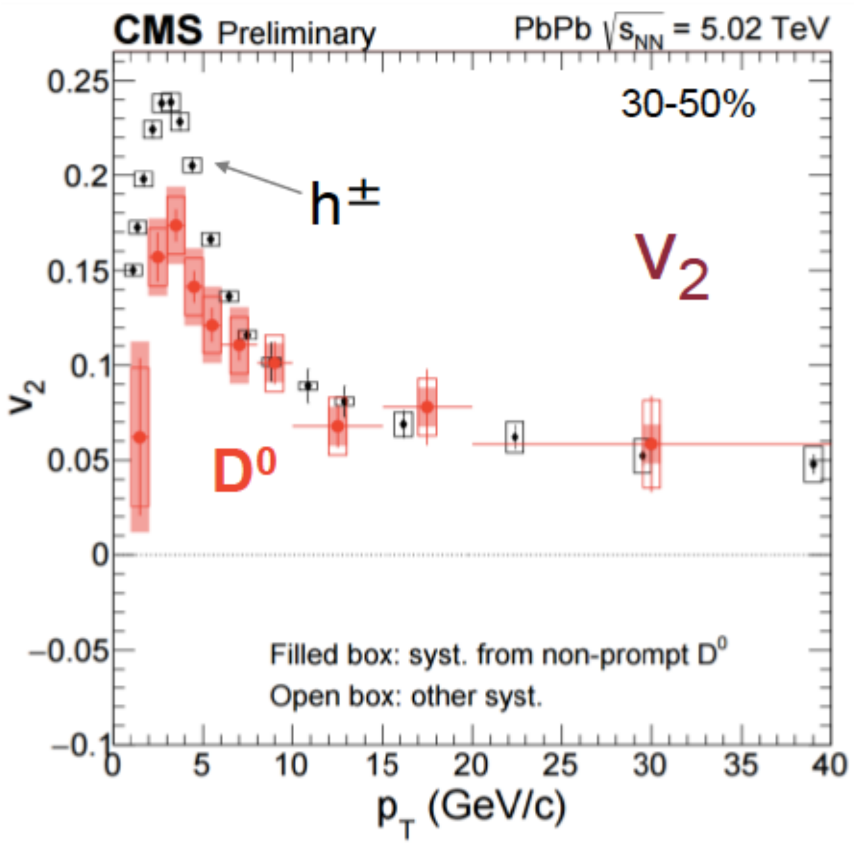

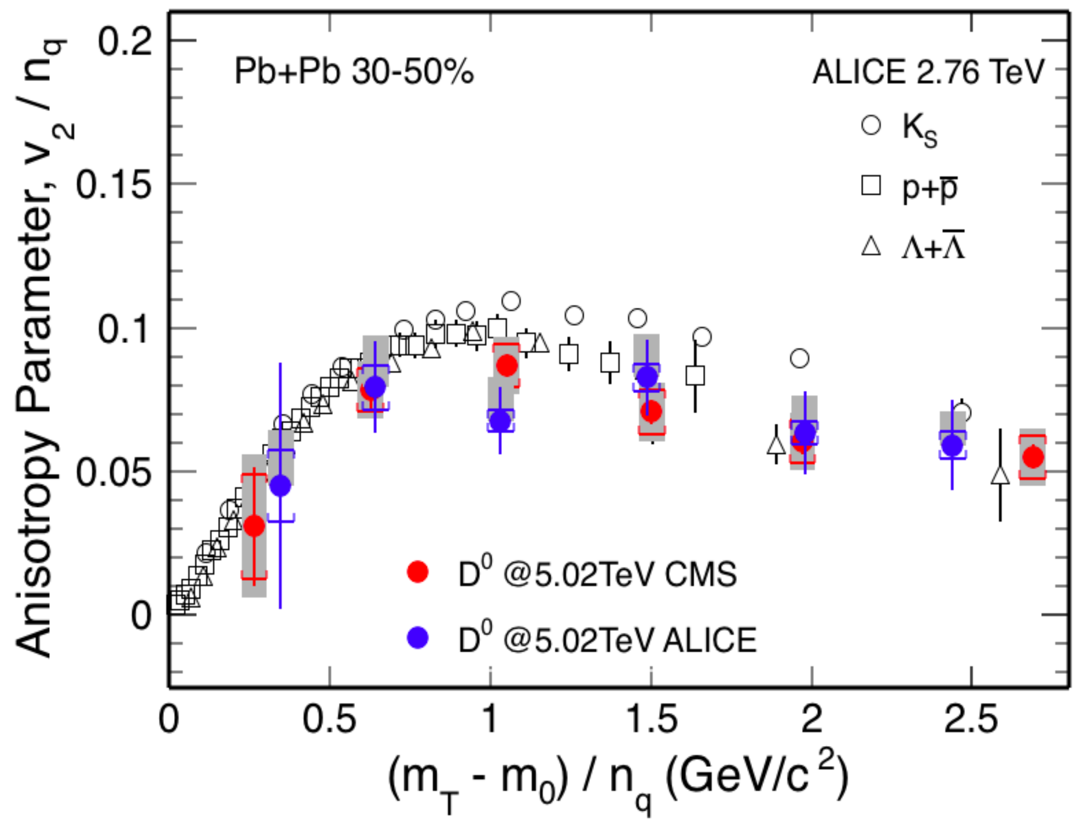

CMS-HIN-16-007; ALICE, 1804.09083

ALICE 2.76 TeV data: JHEP 06 (2015) 190

- Significant D-meson v_2 at 5.02 TeV Pb+Pb collisions
- D^0 v_2 follows the same trend as light hadrons at LHC

Charm Quark Hadronization – Λ_c

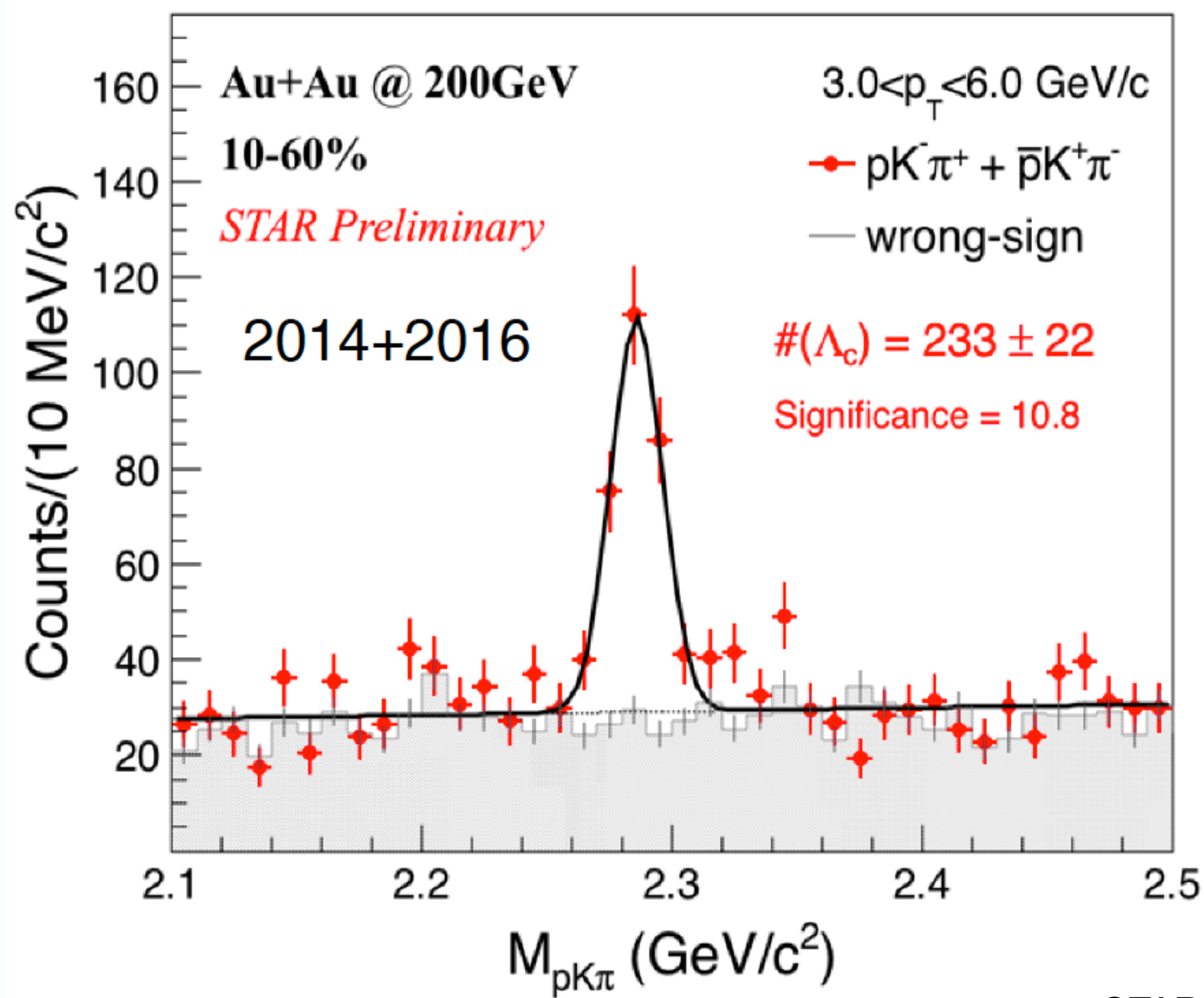

STAR, QM18

$\Lambda_c^+ \rightarrow pK^-\pi^+$

$c\tau = 60\,\mu m$

- Λ_c reconstructed first time in A+A collisions

Λ_c Enhancement in Heavy Ion Collisions

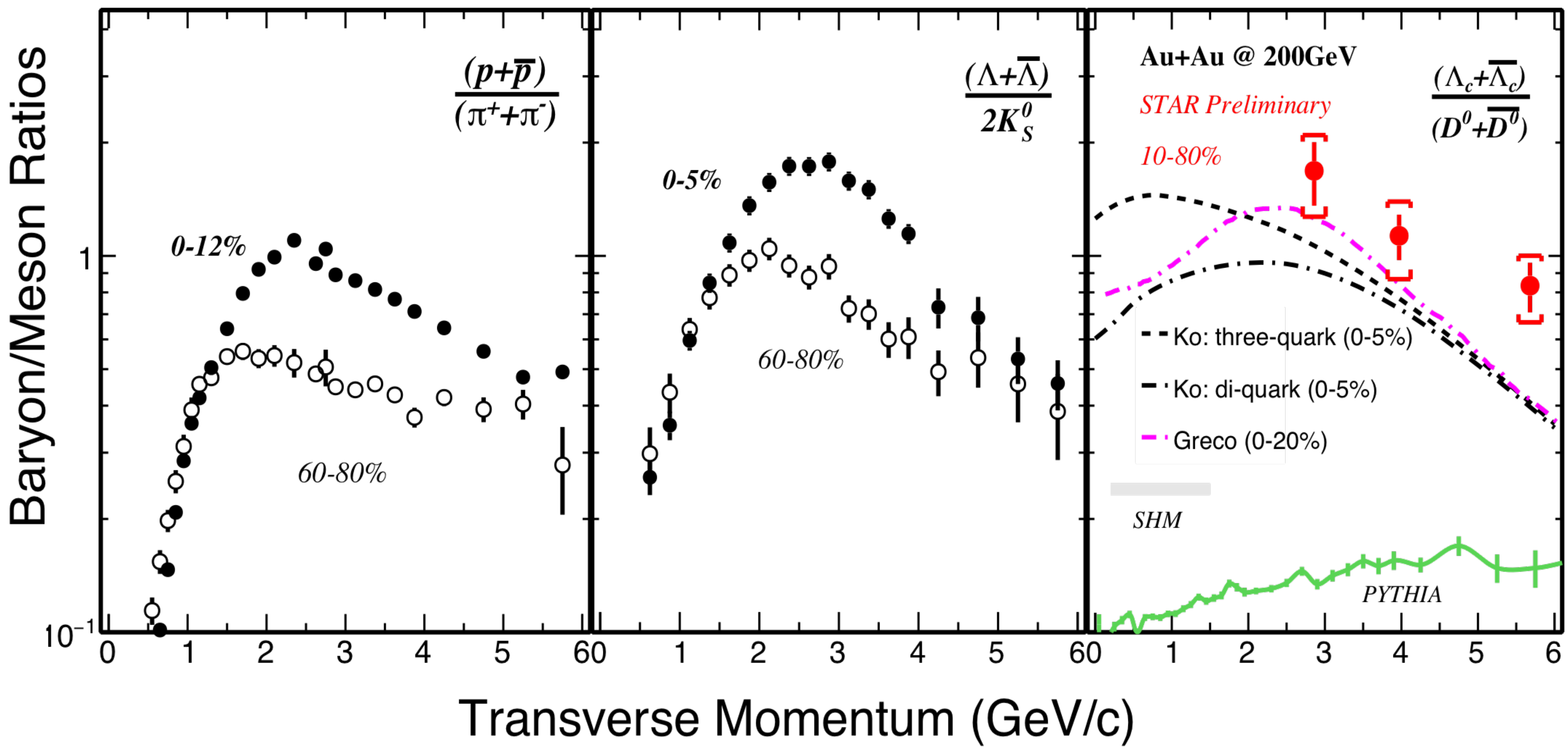

Ko model : Y. Oh, et.al. PRC 79 (2009) 044905; Greco model : S.Plumari, et. al. EPJC 78 (2018) 348

- Significant enhancement in Λ_c/D compared to PYTHIA/fragmentation baseline
- The Λ_c/D^0 ratio is compatible with light flavor baryon-to-meson ratios
- Consistent with coalescence + thermalized charm quarks

Summary - Charm

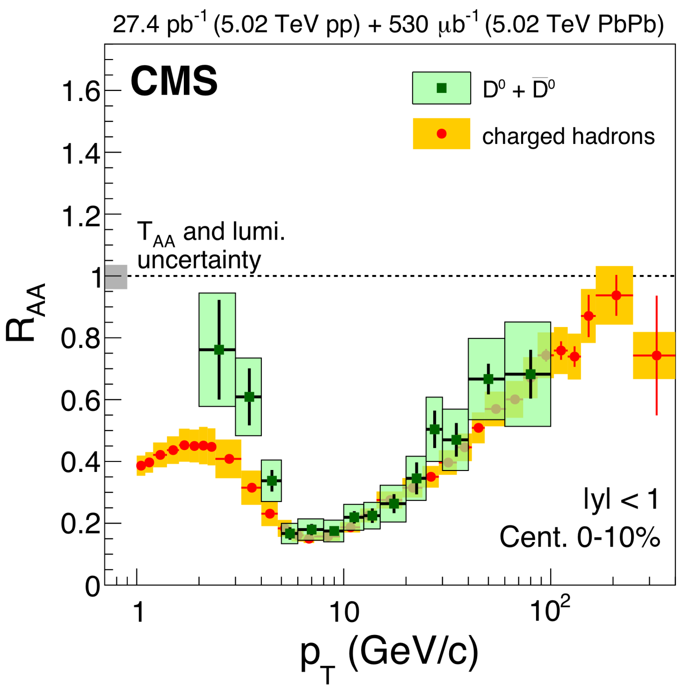

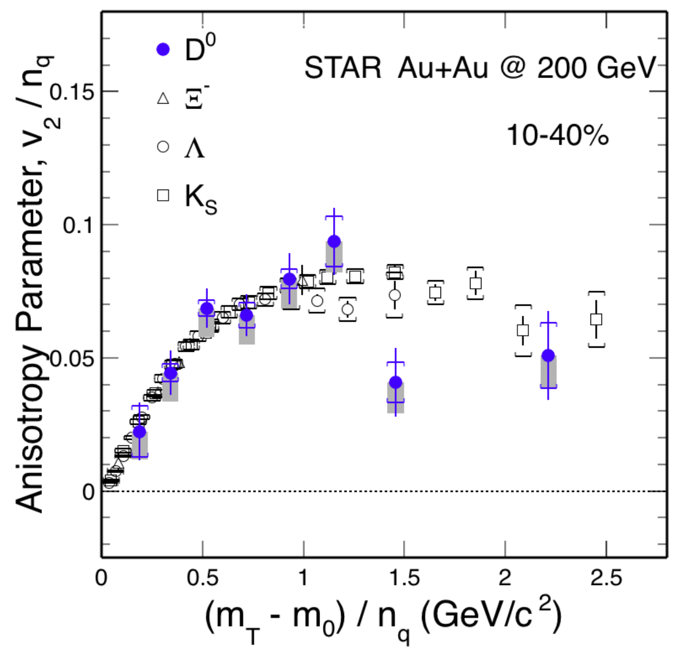

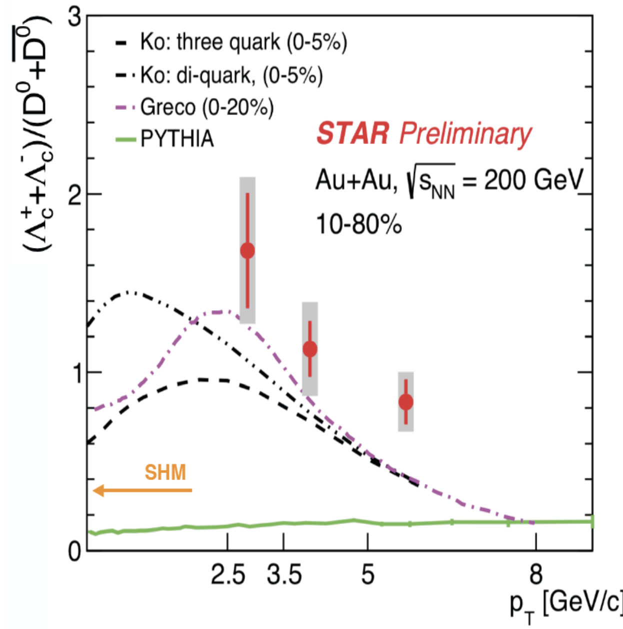

$R_{AA}(D) \sim R_{AA}(h)$ (p_T>5 GeV/c)	- charm quarks lose significant energy
$v_2(D) \sim v_2(h)$ vs. m_T	- charm quarks flow like light quarks
Λ_c/D^0 and D_s/D^0 enhancement	- coalescence hadronization

Charm quarks very strongly coupled with QGP

Evidence of charm quark flowing with the QGP

Towards Extraction of Heavy Quark Diffusion Coefficient

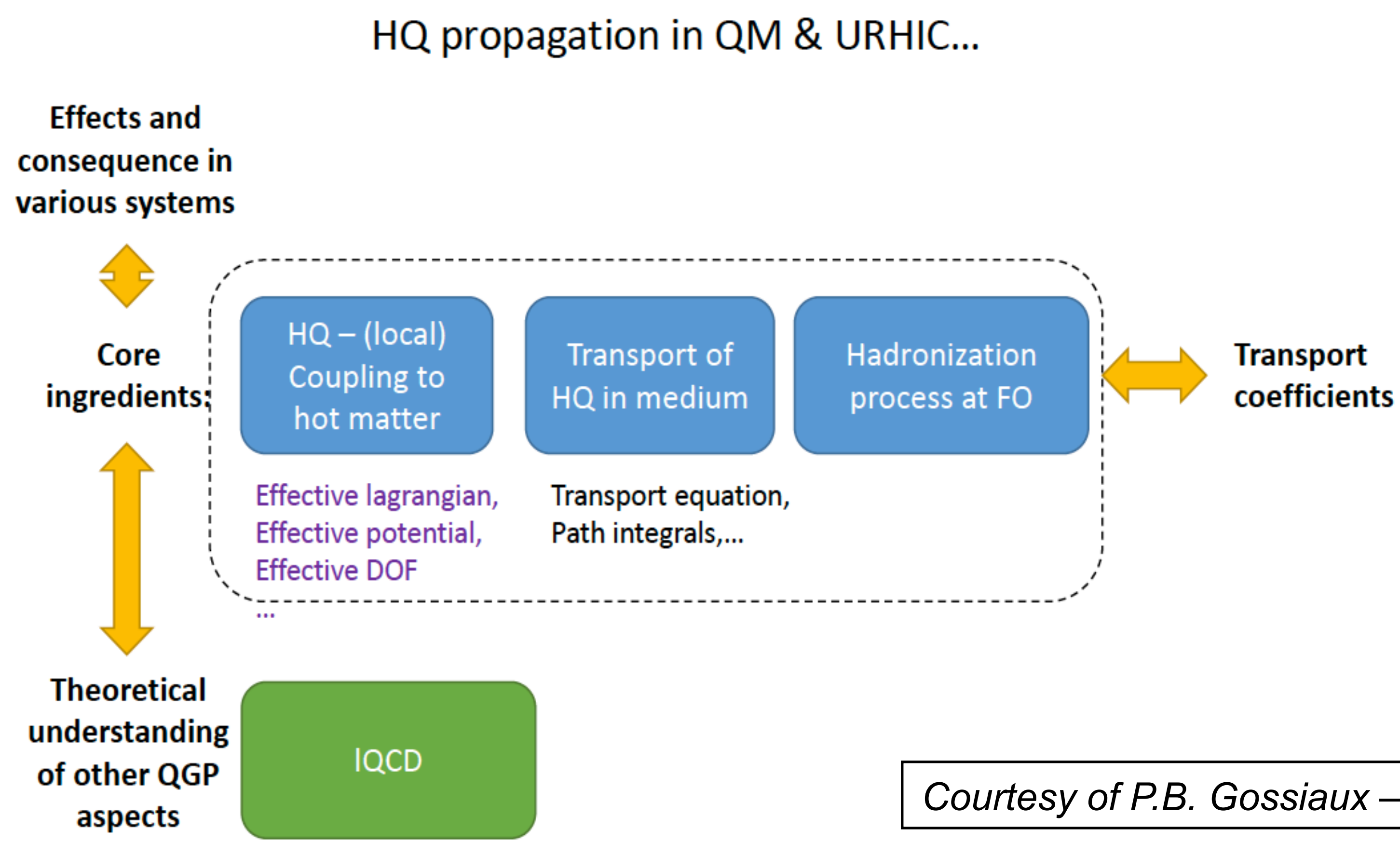

Courtesy of P.B. Gossiaux – QM18

Rapid developments among theorists to understand trivial/non-trivial differences between models/groups

- Heavy Quark Working Group
- EMMI Rapid Response Tasking Force - *R. Rapp et al. 1803.03824*

Bayesian Analysis to Extract HQ Diffusion Coefficient

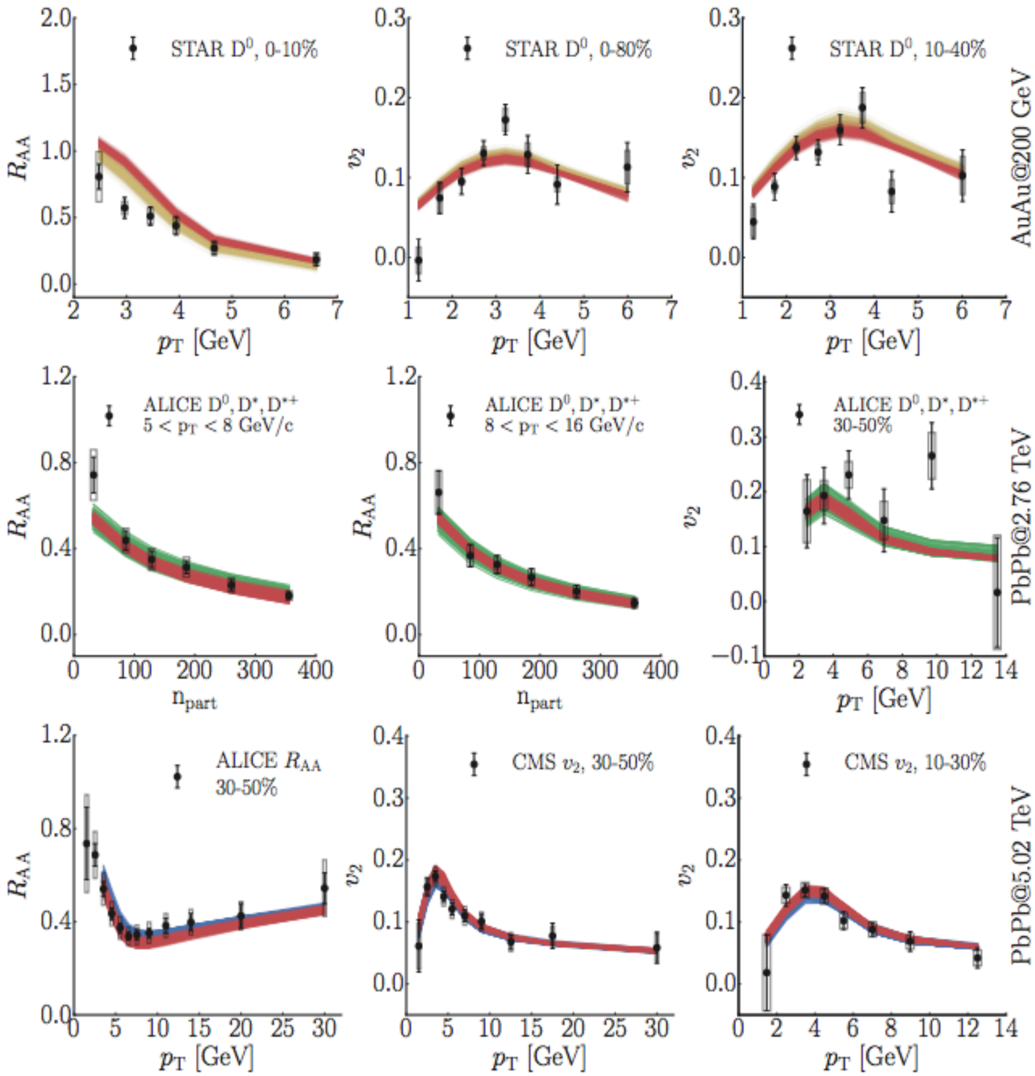

Bayesian analysis based on Duke model:
Langevin + Hydro

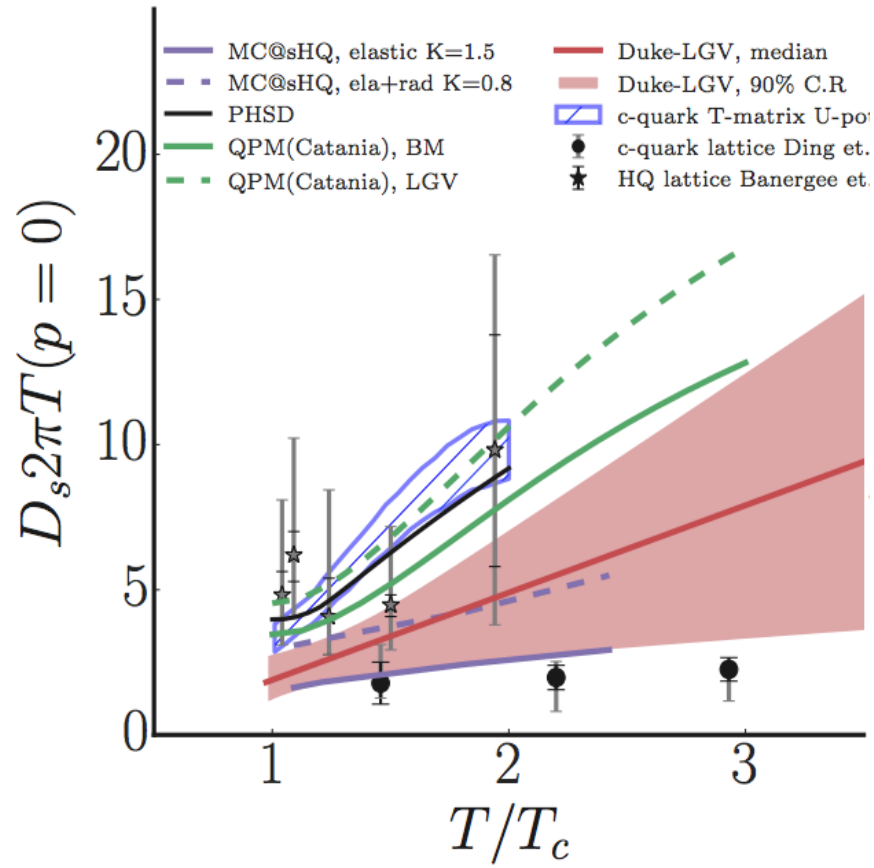

Y. Xu et al, PRC 97 (2018) 014907

Open question: Charm heavy enough ? (as compared to medium interactions)

-> Go Heavier !!!

B-meson and b-jet at high p_T

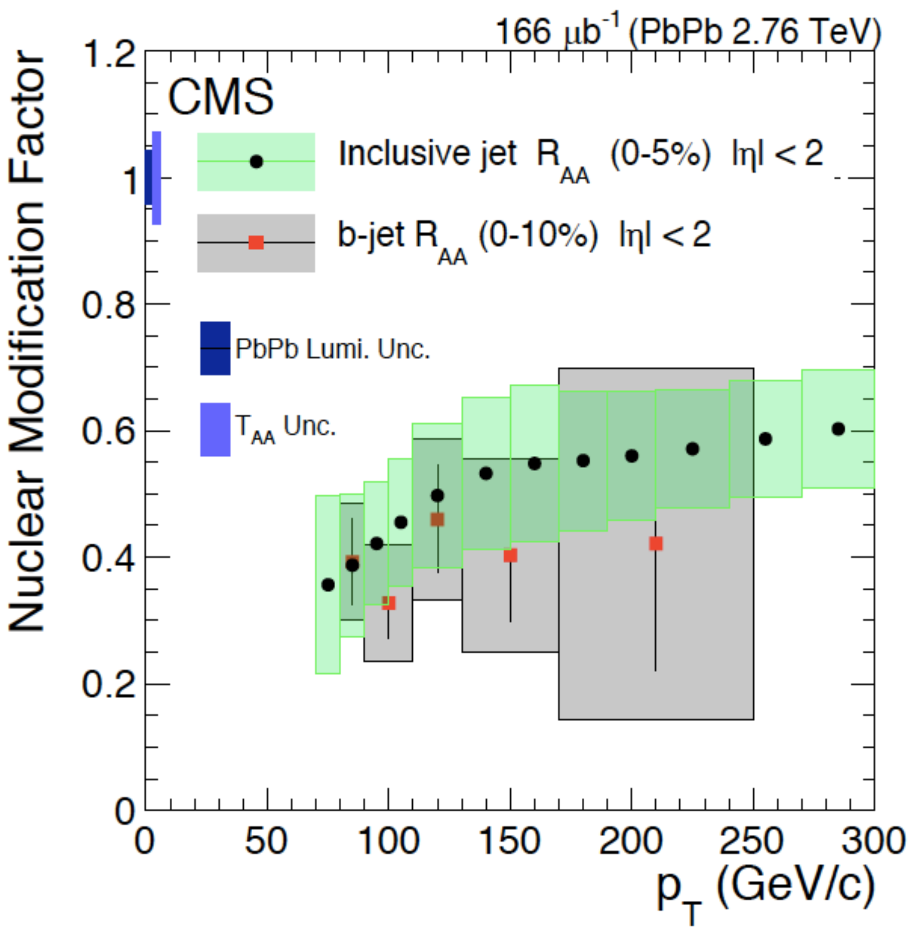

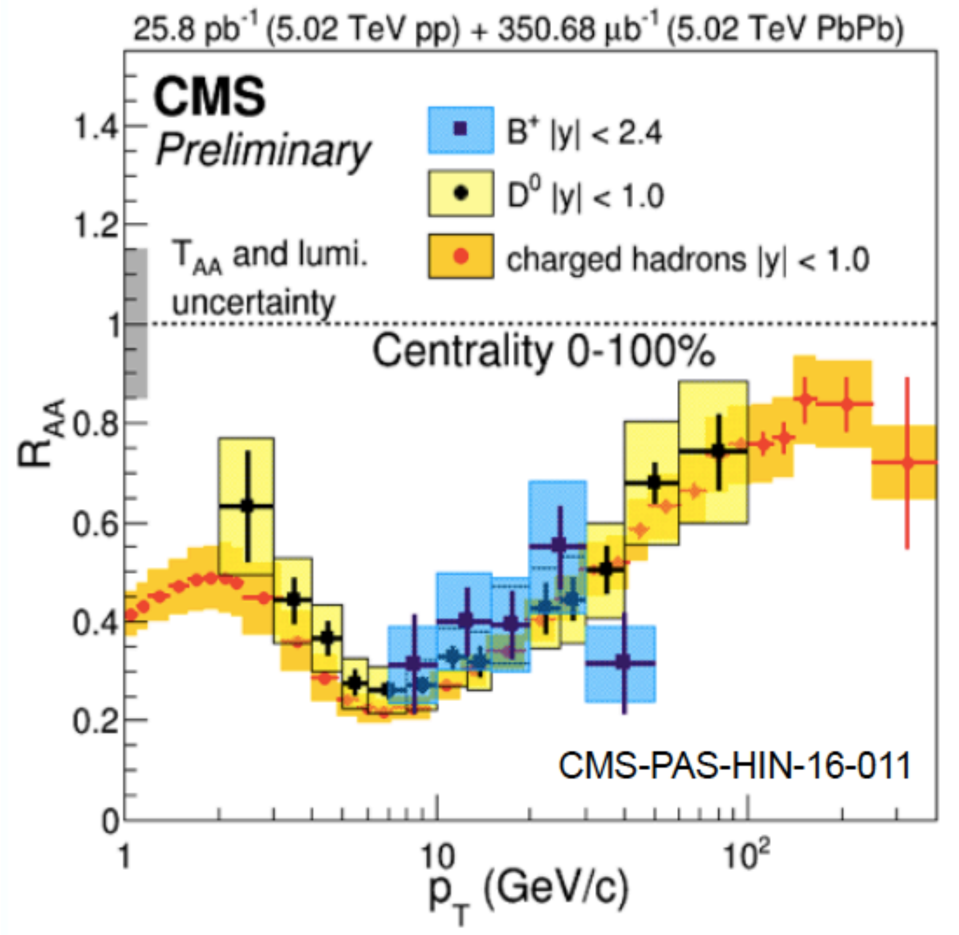

CMS, PRL 113 (2014) 132301, PRL 119 (2017) 152301

- R_{AA}(b-jet) ~ R_{AA}(incl. jet) at p_T > 70 GeV/c
- R_{AA}(B+) ~ R_{AA} (D) ~ R_{AA}(h) at p_T > 10 GeV/c

Mass hierarchy? -> Going to lower p_T

Bottom Suppression at Low p_T at LHC

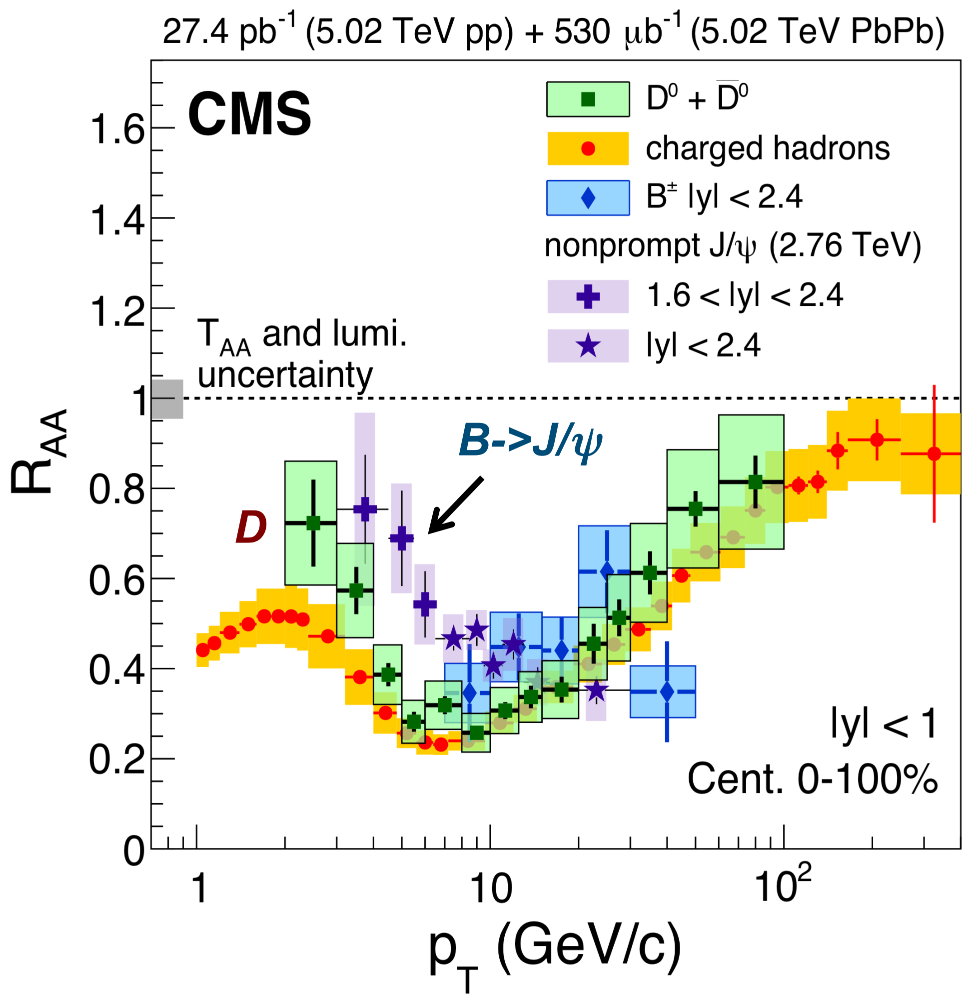

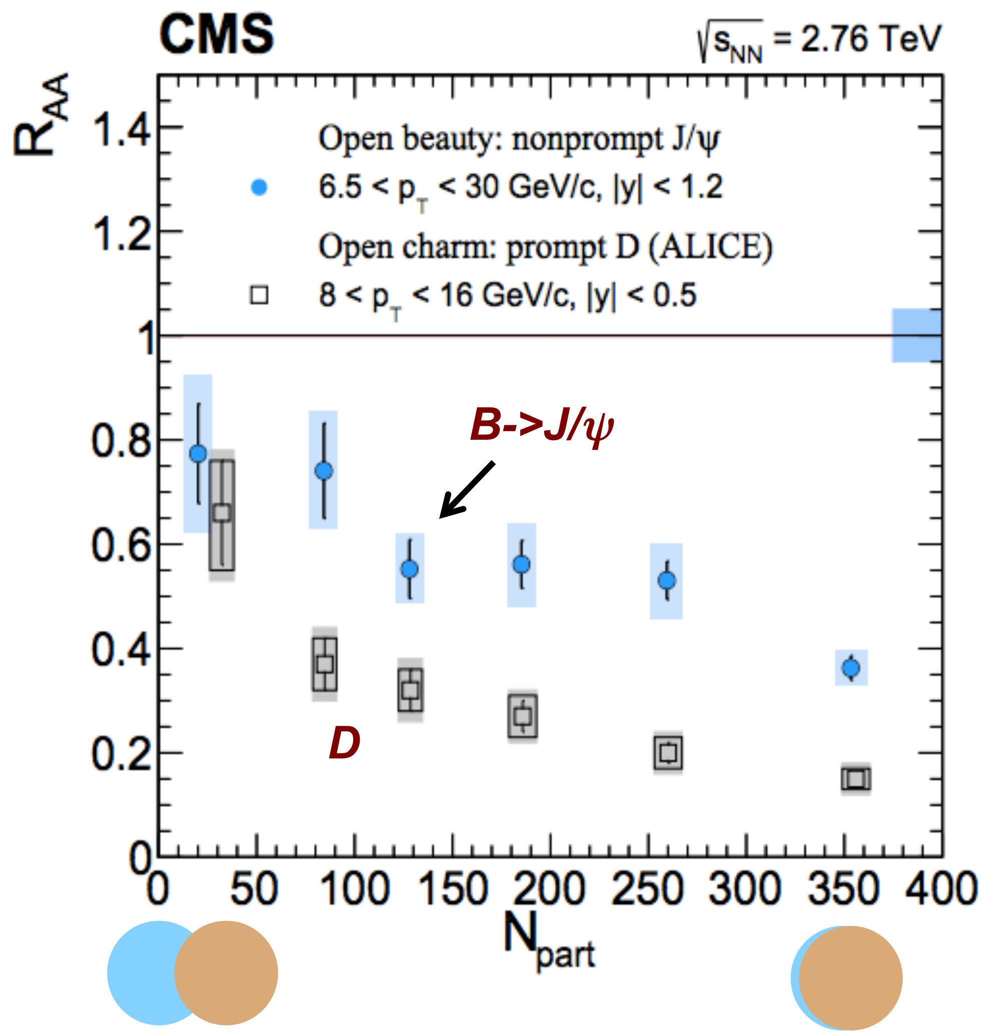

CMS, arXiv: 1708.04962

- $R_{AA}(J/\psi_B) > R_{AA}(D)$ at $p_T < 10$ GeV/c

Evidence of suppression mass hierarchy at low p_T

- consistent with pQCD calculations

Bottom Measurements at RHIC

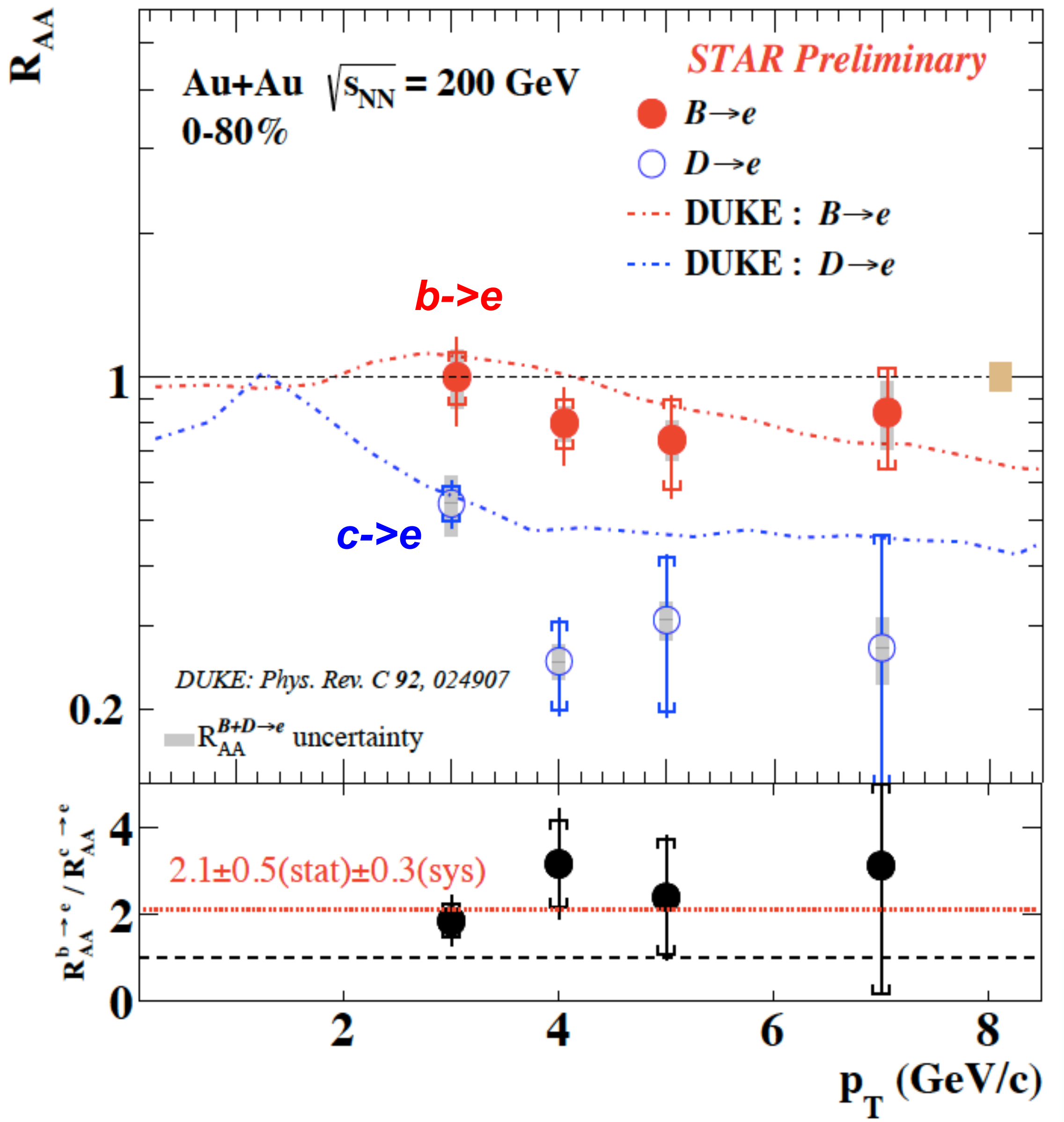

STAR, QM17

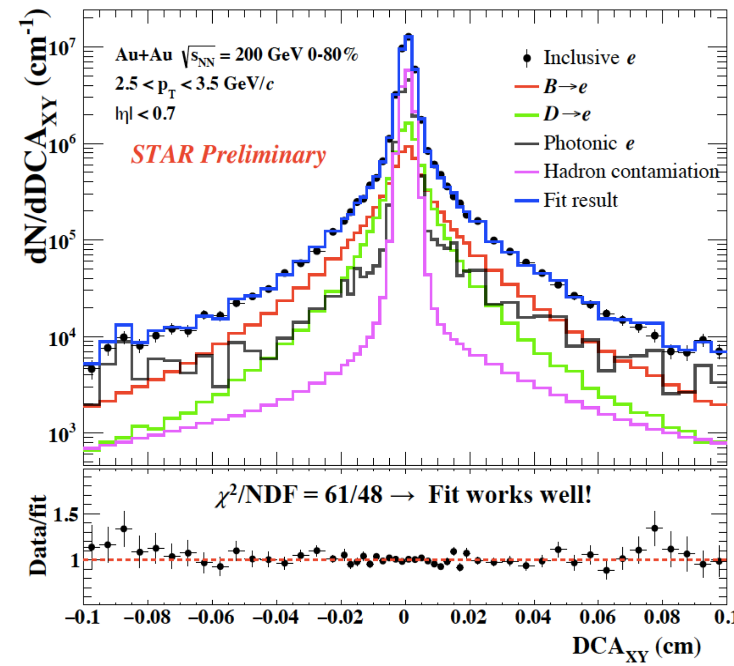

Impact parameter method to separate c/b electrons and non-prompt D^0, J/ψ

• $R_{AA}(e_B) < R_{AA}(e_D)$ at 3 – 8 GeV/c (2σ)

mass hierarchy of parton energy loss

Summary - Bottom

LHC 2.76 TeV

$R_{AA}(J/\psi_B) > R_{AA}(D)$

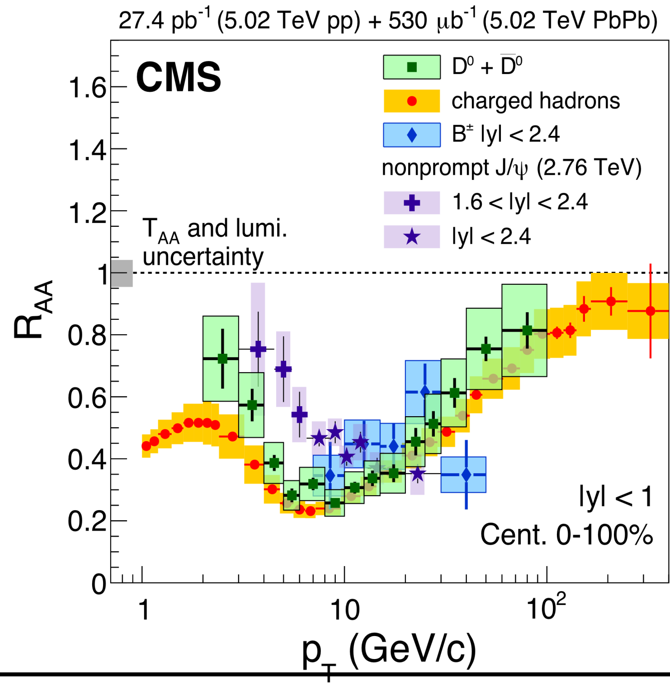

RHIC 200 GeV

$R_{AA}(e_B) > R_{AA}(e_D)$

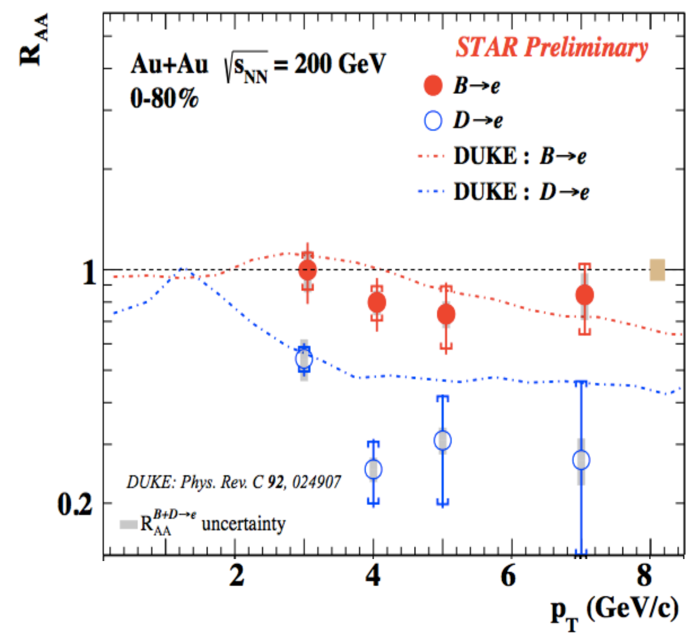

- R_{AA} (B^+, *b*-jet, non-prompt J/ψ's) ~ R_{AA} (h,jet) at p_T > 10 GeV/c
- R_{AA} (non-prompt J/ψ's, e_B) > R_{AA} (D, e_D) at p_T < 10 GeV/c

Evidence of less energy loss of bottom in the QGP
- mass hierarchy of parton energy loss !

Precision low p_T bottom measurements (R_{AA}, v_2)
- to quantify medium transport parameter

Future – Precision Open Bottom Measurements

Precision bottom (B-meson and *b*-jet) measurements

next generation fast MAPS detector with high luminosity heavy ion runs

- systematic investigation of mass dependence of parton energy loss
- precision determination of heavy quark diffusion coefficient

ITS upgrade at ALICE, MVTX@sPHENIX (~ 2020+)

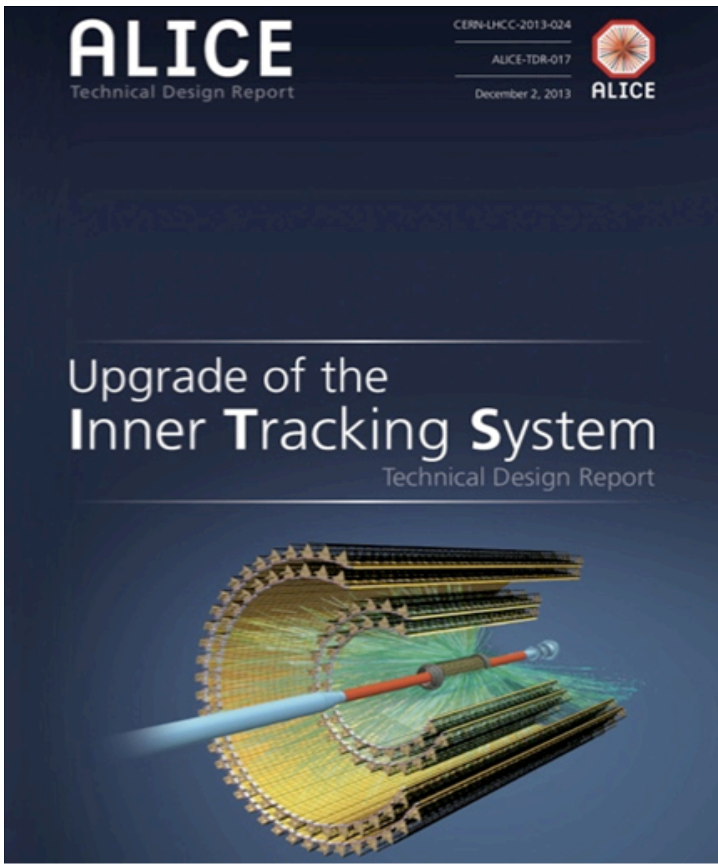

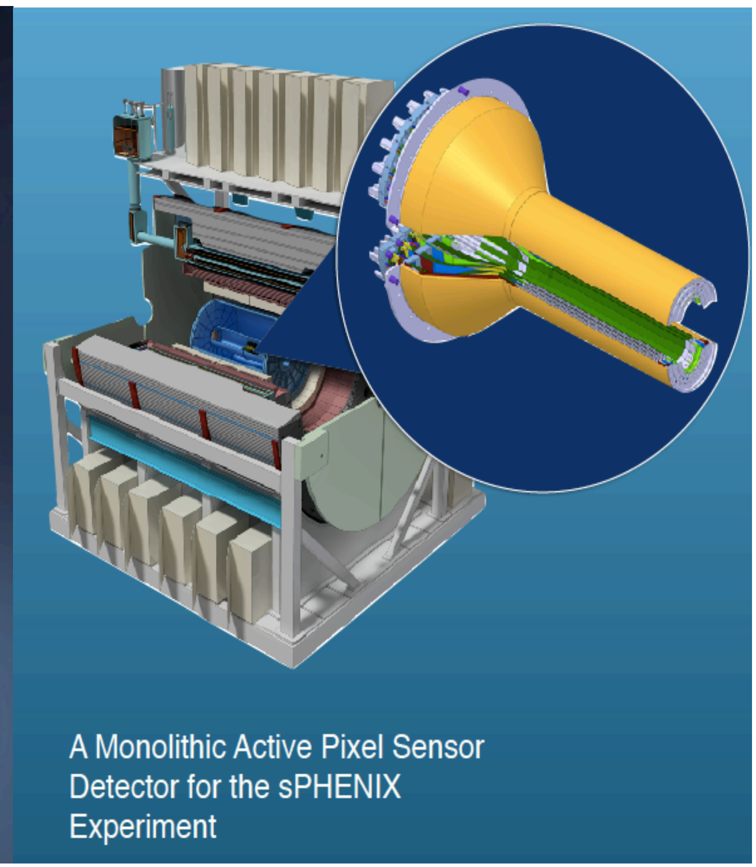

1900s

Microscope

Brownian motion kinetic theory

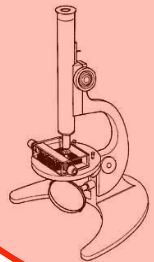

$$\frac{\partial\rho}{\partial t} = D\frac{\partial^2\rho}{\partial x^2}$$

1950s-1970s

Bubble chamber

Yang-Mills -> QCD theory

$$\mathcal{L}_{\mathrm{QCD}} = \bar{\psi}_i \left(i(\gamma^\mu D_\mu)_{ij} - m\,\delta_{ij} \right) \psi_j - \frac{1}{4} G^a_{\mu\nu} G^{\mu\nu}_a$$

2000s-2020s

MAPS at RHIC/LHC

Femtoscopic "Brownian" motion to investigate hot QCD matter

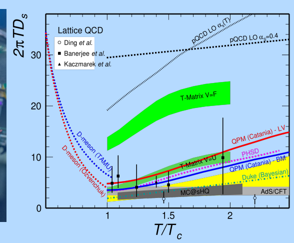

"Cutting edge experimental research is largely defined by new technology"

- C.N. Yang, 2017

Backups

Quark-Gluon Plasma – "Perfect Liquid"

State-of-the-art viscous hydrodynamic simulations

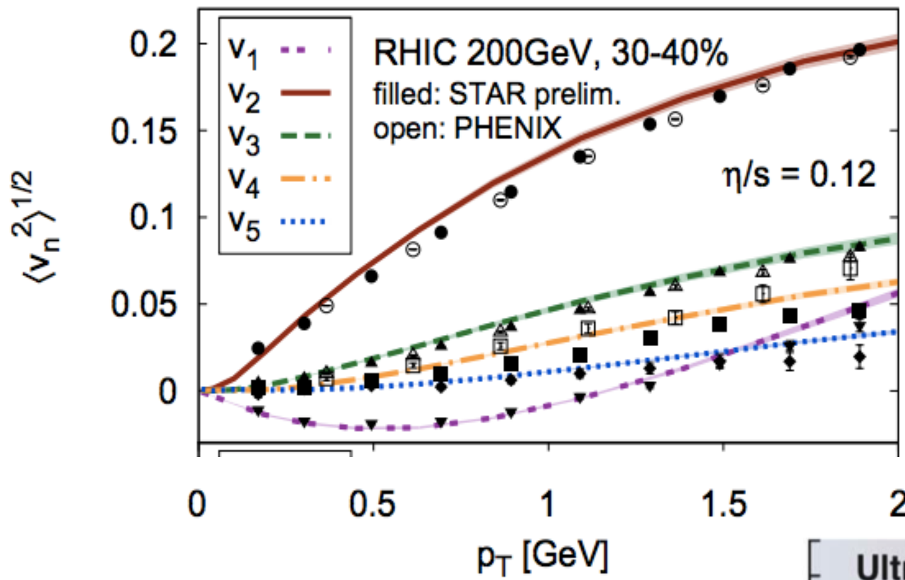

Gale et al., PRL 110 (2012) 012302

"Perfect liquid"

- strongly coupled (not gas)
- low viscosity (transporting particles freely)

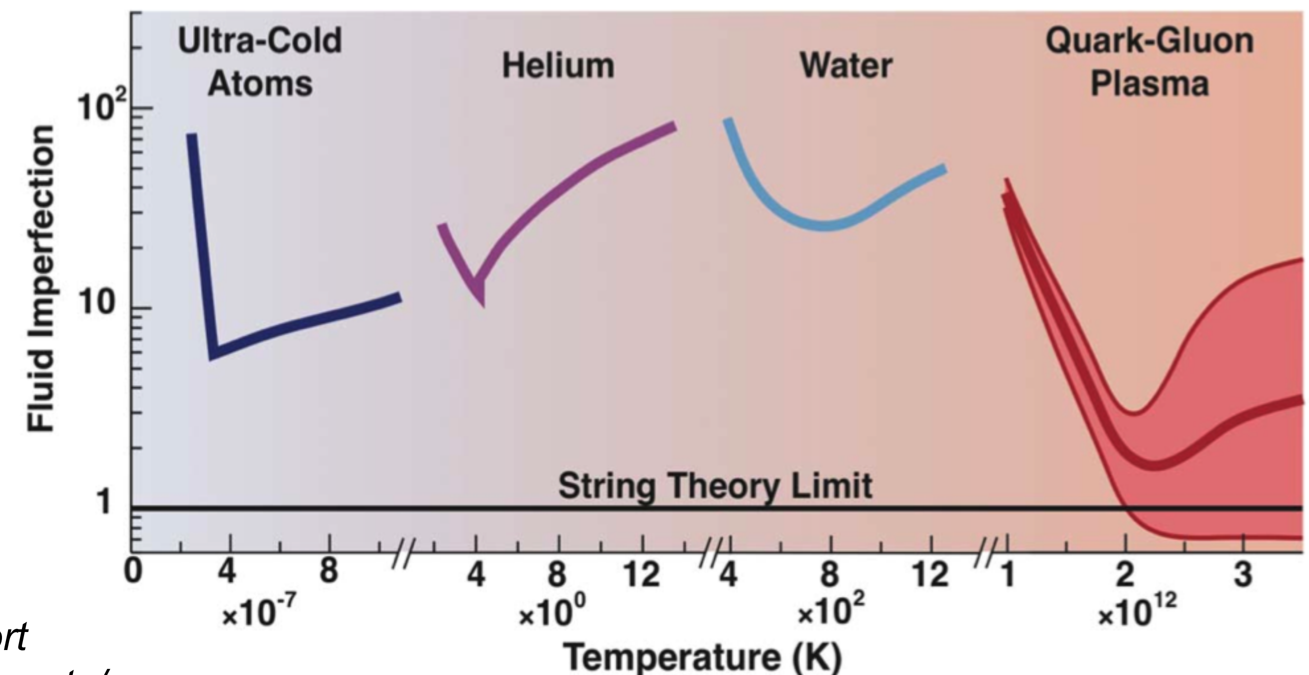

2013 NSAC Tribble Committee report
http://science.energy.gov/np/nsca/reports/

Charm Production in p+p Collisions

0.2-7 TeV mid-rapidity

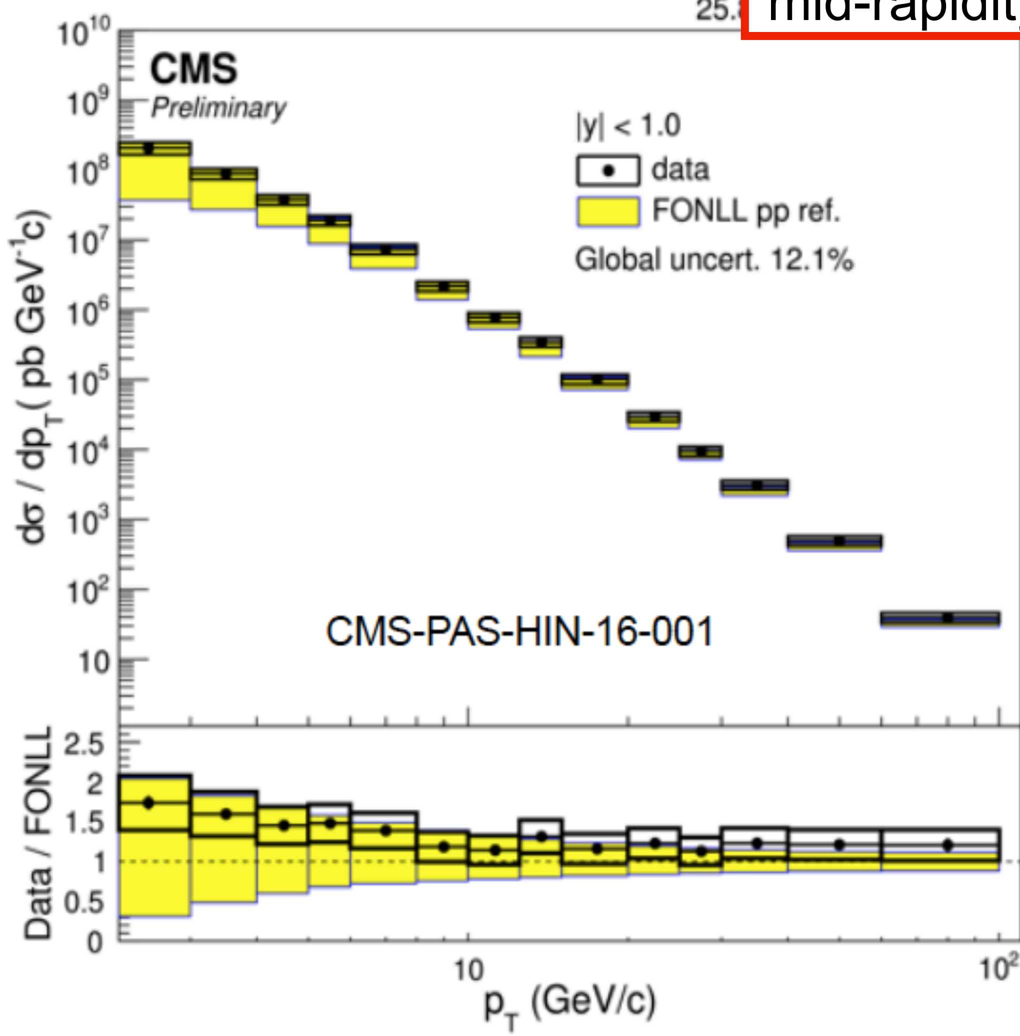

13 TeV forward-rapidity

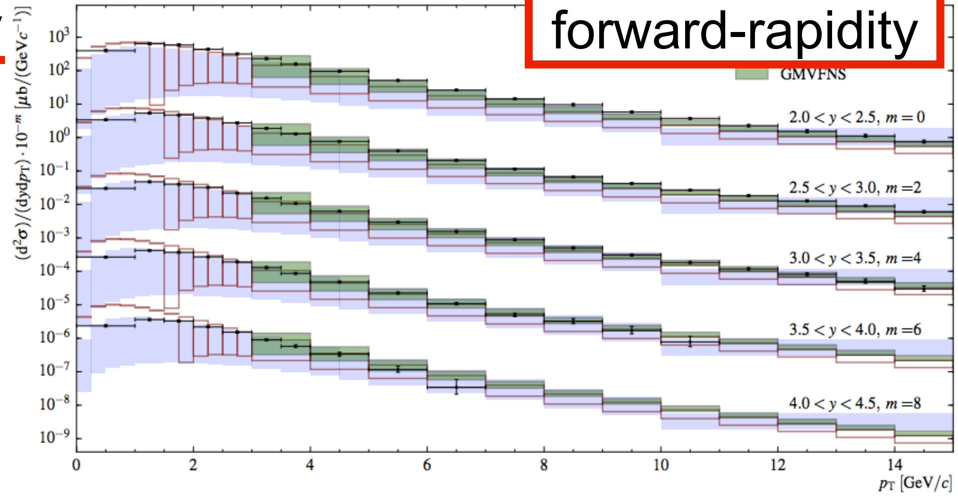

STAR, PRD 86 (2012) 072013, QM14
CDF, PRL 91 (2003) 241804
ALICE, JHEP 01(2012) 128, EPJC 77 (2017) 550
LHCb, JHEP 03 (2016) 159, 09 (2016) 013

- Charm hadron spectra well described by pQCD FONLL
  - data prefer upper bounds of FONLL calculations

D_s Enhancement in Heavy Ion Collisions

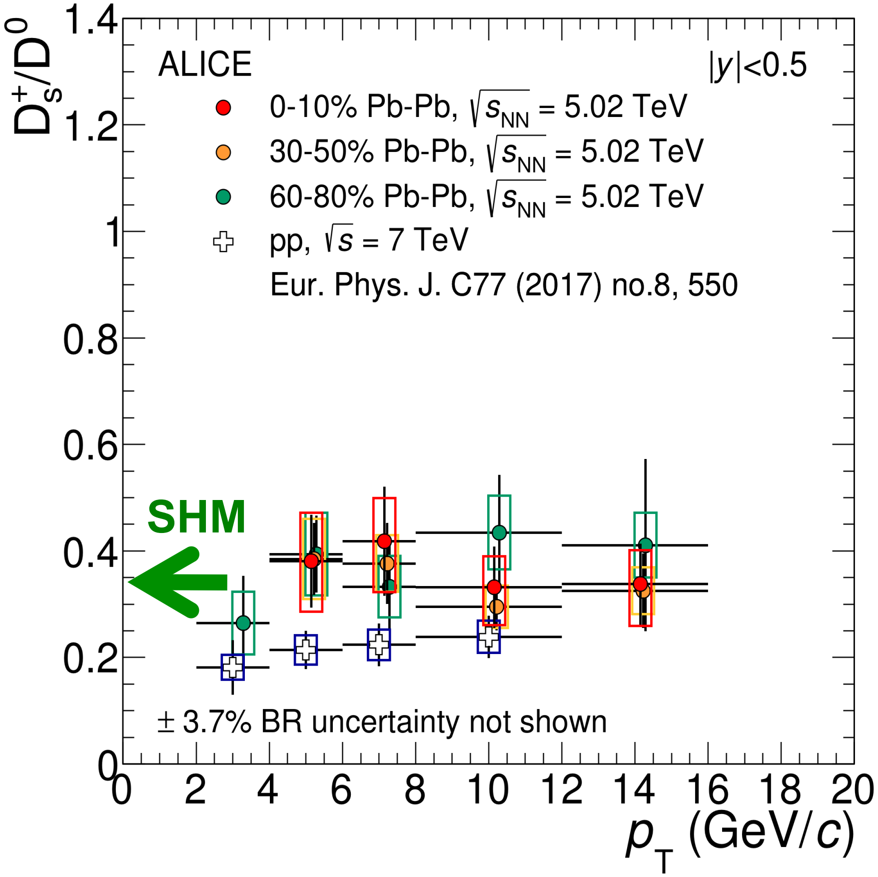

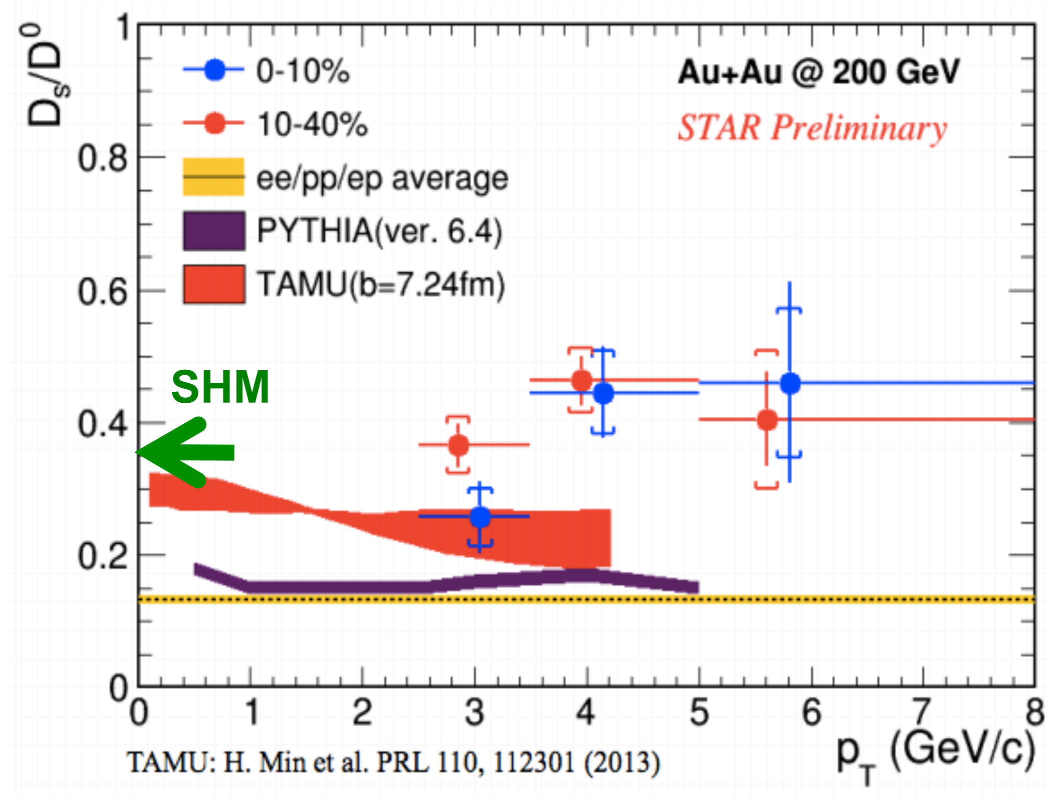

ALICE, arXiv: 1804.09083; STAR QM17

• D_s/D^0 enhancement in mid-central Au+Au and Pb+Pb collisions w.r.t fragmentation baseline or p+p measurement

- Coalescence hadronization
- Statistical Hadronization Model predicts D_s/D^0 ratio ~ 0.35-0.40 (central)

A. Andronic et al., PLB 571 (2003) 36

Bottom Production in p+p Collisions

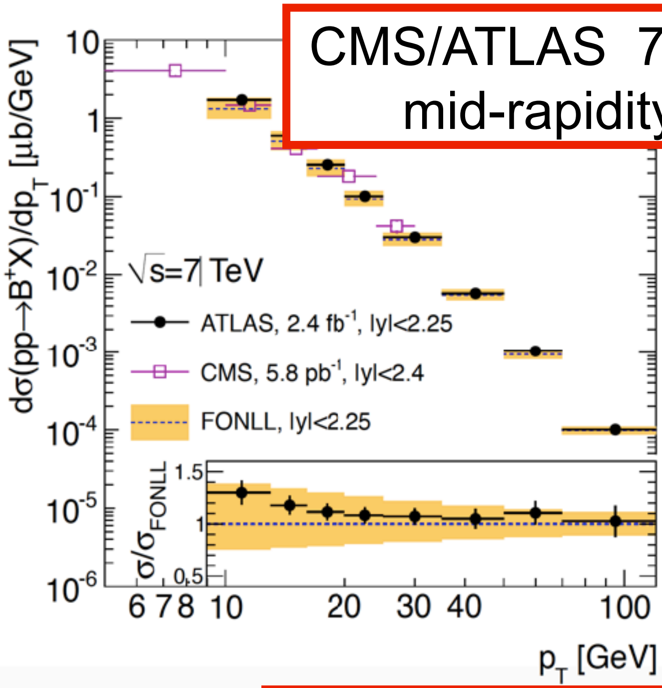

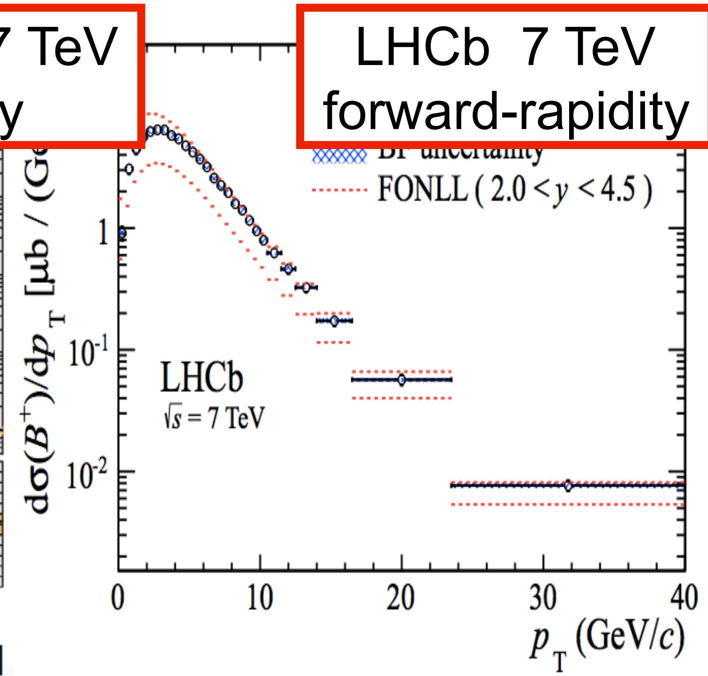

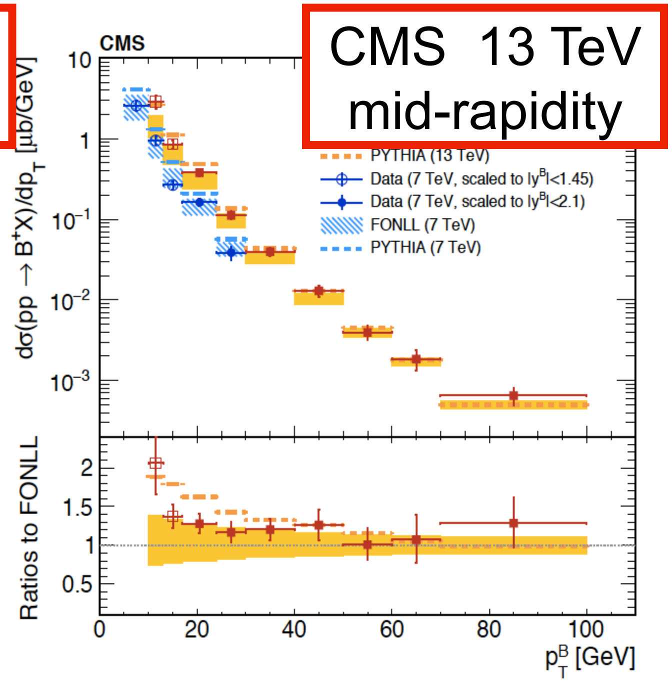

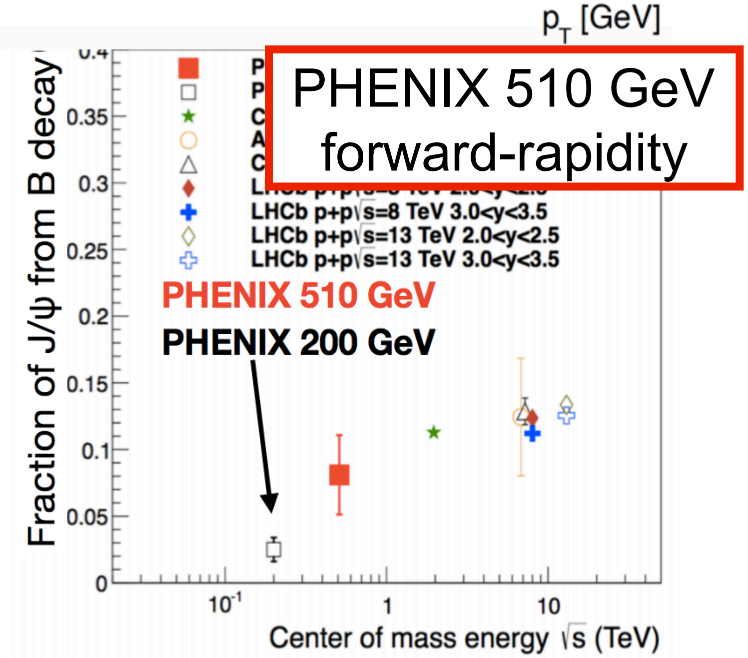

CMS, PRL 106 (2011) 112001; ATLAS, JHEP 10 (2013) 042; LHCb, JHEP 08 (2013) 117; CMS, arXiv: 1609.00873; PHENIX, arXiv: 1701.01342

- pQCD FONLL calculations describe the bottom production
  - consistent with FONLL central values at p_T > 20 GeV/c (CMS/ATLAS)

Relativistic Heavy Ion Collider (RHIC)

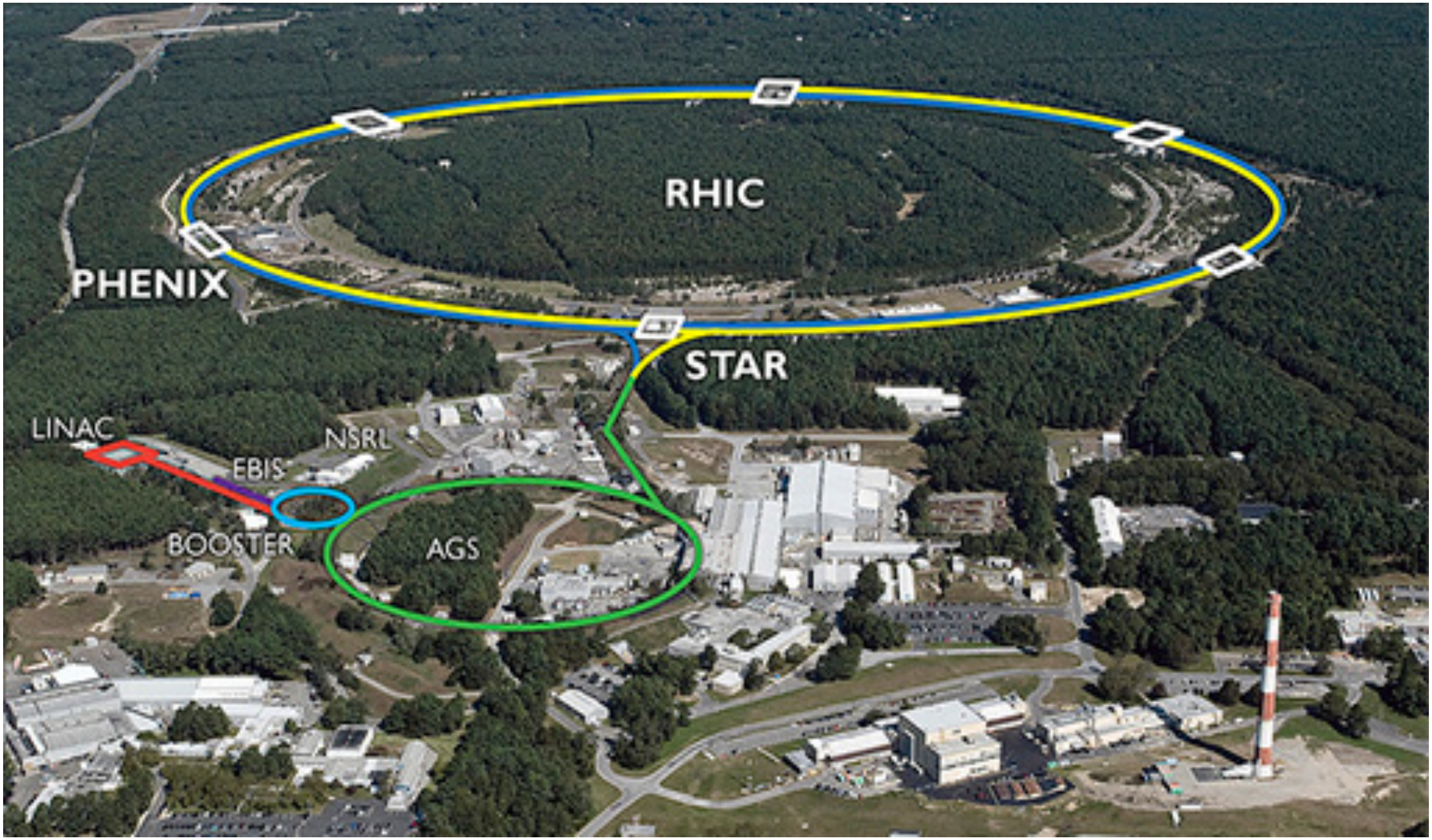

- Successfully operated for 17 years since 2000
- Beam species from proton to Uranium,
  7.7 – 200 GeV (ions) / 510 GeV (polarized protons)

Heavy Flavor Tracker for STAR

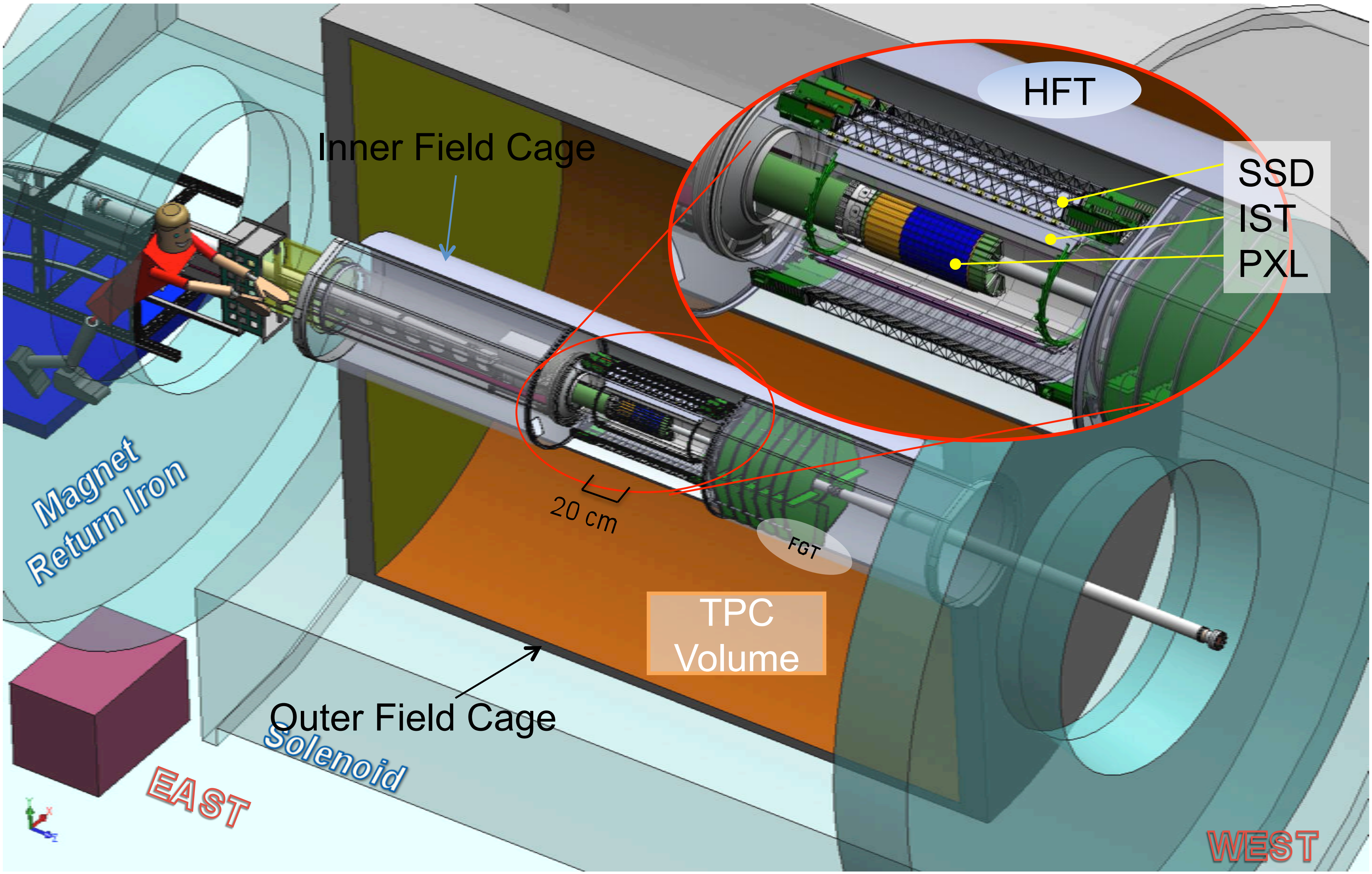

Heavy Flavor Tracker for STAR

- HFT consists of 3 sub-detector systems inside the STAR Inner Field Cage

Detector	Radius (cm)	Hit Resolution R/φ - Z (μm - μm)	Thickness
SSD	22	30 / 860	1% X_0
IST	14	170 / 1800	1.32 %X_0
PIXEL	8	6.2 / 6.2	~0.52 %X_0
	2.8	**6.2 / 6.2**	**~0.39% X_0**

➢ **SSD** existing single layer detector, double side strips (electronic upgrade)

➢ **IST** one layer of silicon strips along beam direction, guiding tracks from the SSD through PIXEL detector - proven pad technology

➢ **PIXEL** double layers, Monolithic Active Pixel Sensor (MAPS), 20.7x20.7 μm^2, 0.4%X_0 thick per layer, air cooled

– first application of MAPS technology at a collider experiment

Charm Hadron v_2 Compared to Models

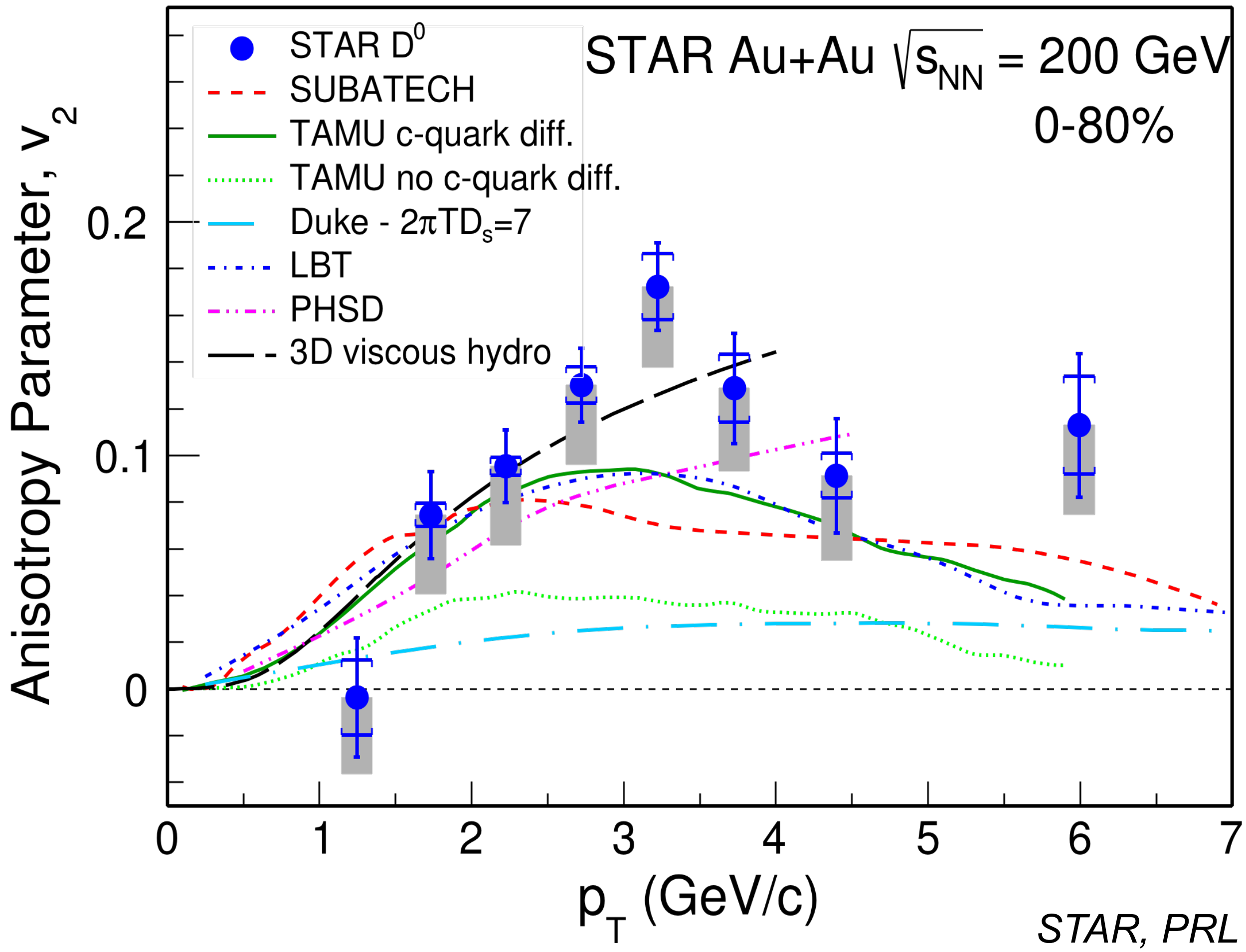

STAR, PRL 118 (2017) 212301

- 3D viscous hydro model calculations describe the D^0 v_2 at p_T< 3-4 GeV/c
  - **Indication of charm quark thermalization in the QGP**
- Data precision good enough to constrain model calculations

R_{AA} and v_2 Compared to Models

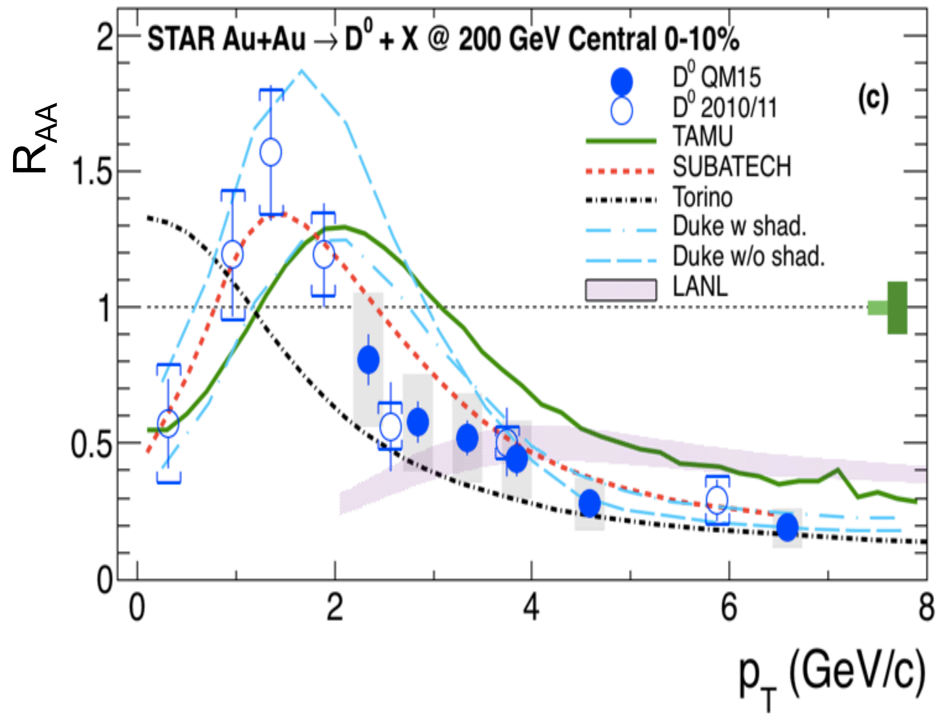

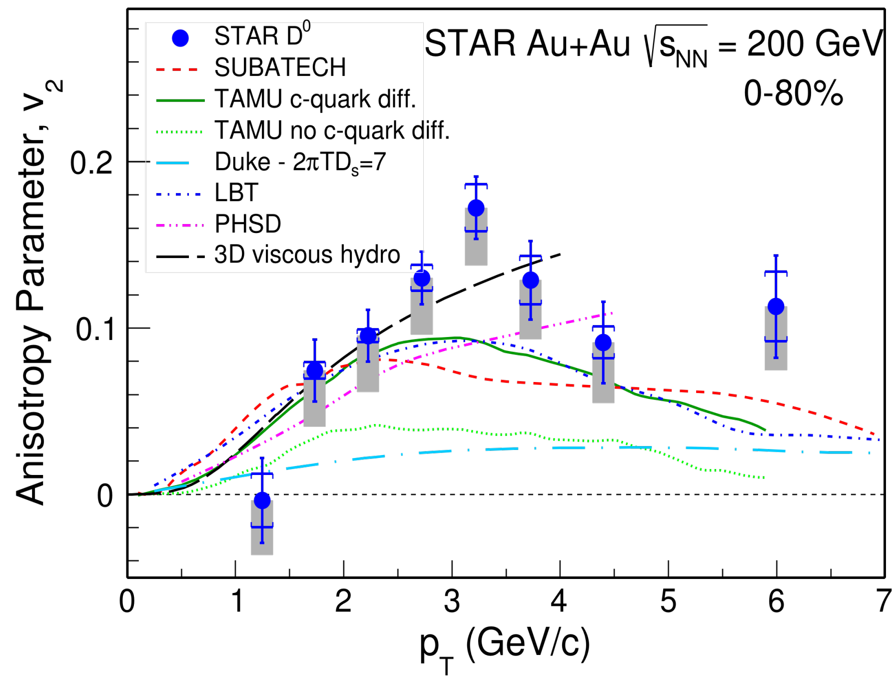

- Understand the trivial/non-trivial differences between models
- Precision data starts to provide constraints on medium transport parameter
  - e.g. Bayesian analysis

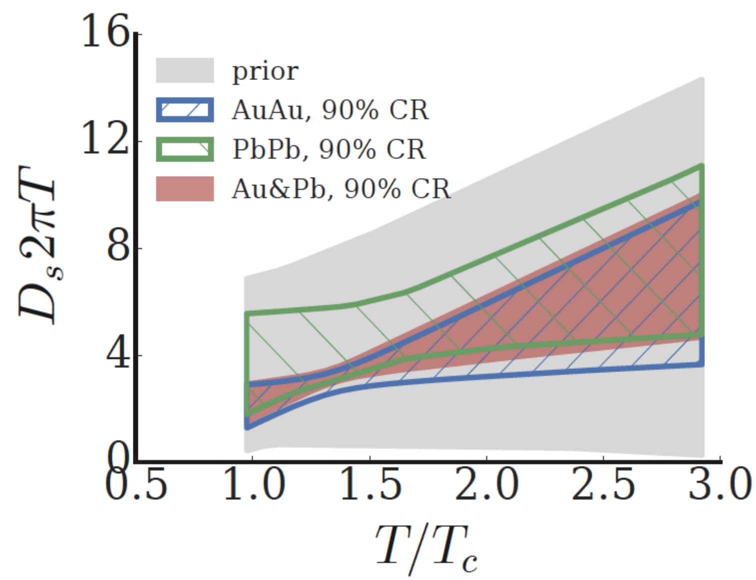

Charm Hadron v_2 Compared to Models

STAR 200 GeV

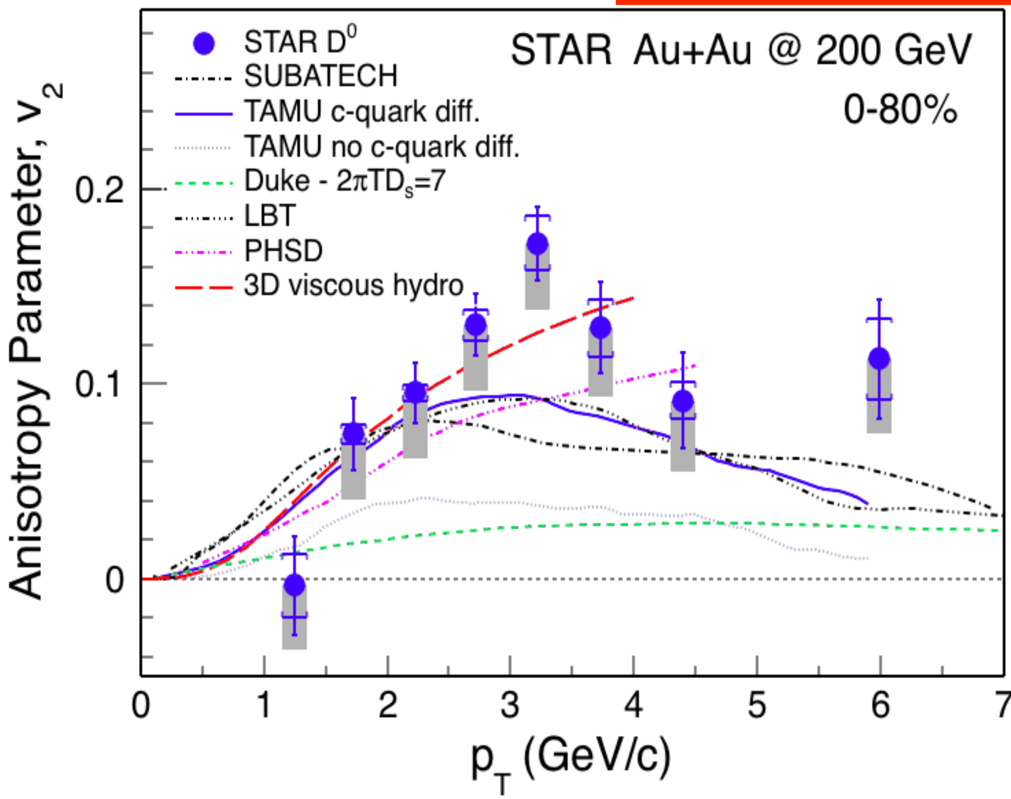

CMS 5.02 TeV

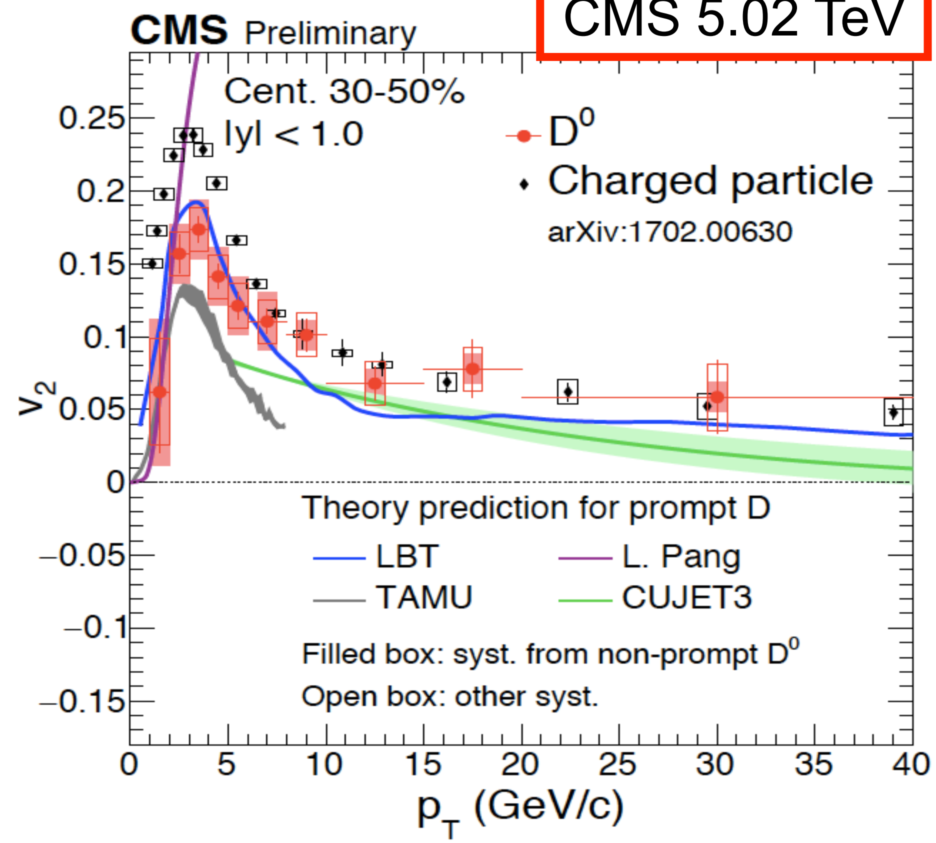

- 3D viscous hydro model calculations describe the D^0 v_2 at p_T< 3-4 GeV/c
  - **Indication of charm quark thermalization in the QGP**
- Data precision good enough to constrain model calculations

Charm Flowing - Next Steps

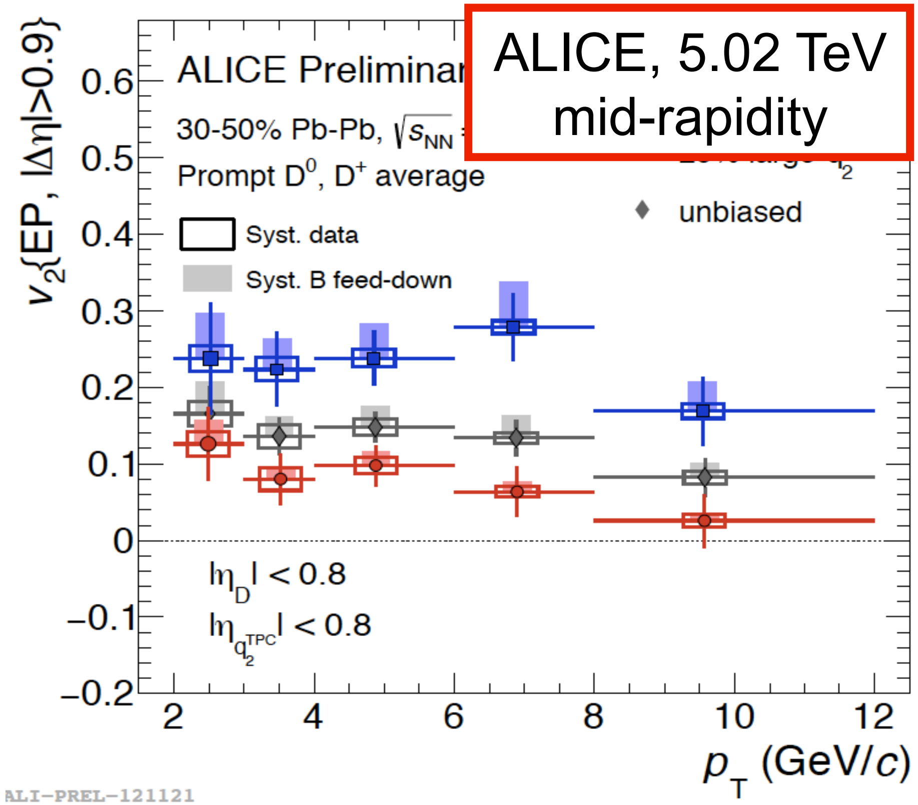

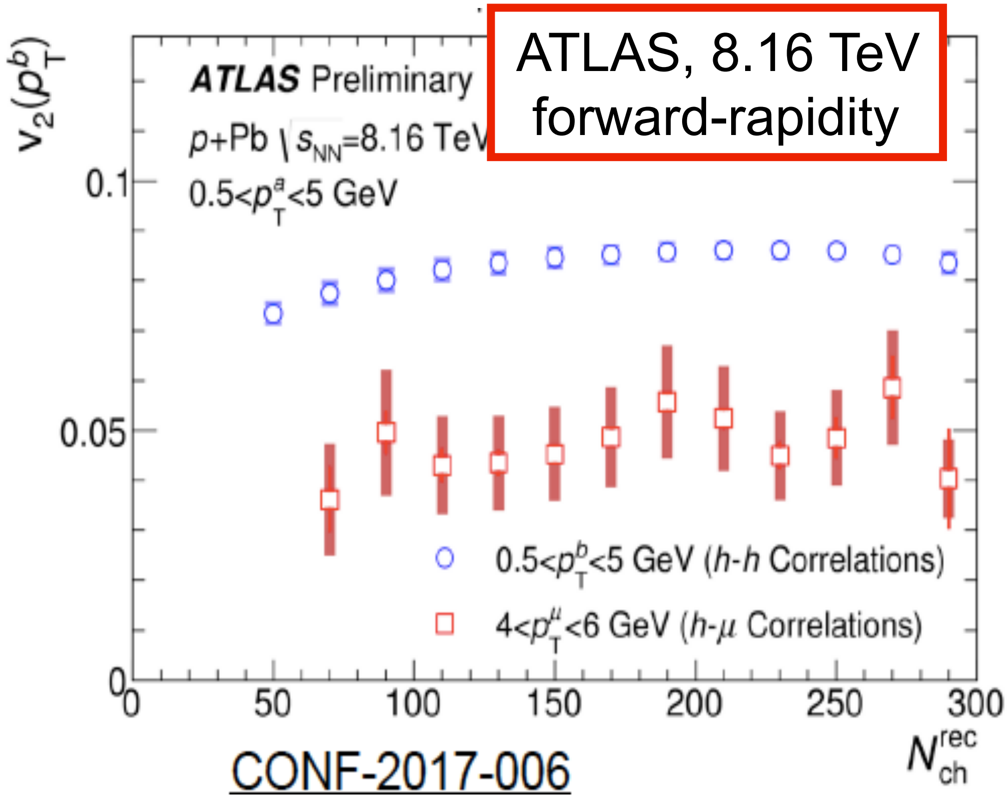

- How do charm quarks reach thermal equilibrium?
  - Correlation with light hadrons
  - Charm quark collectivity in small system

Bottom Electron R_{AA} at RHIC

PHENIX, 200 GeV mid-rapidity

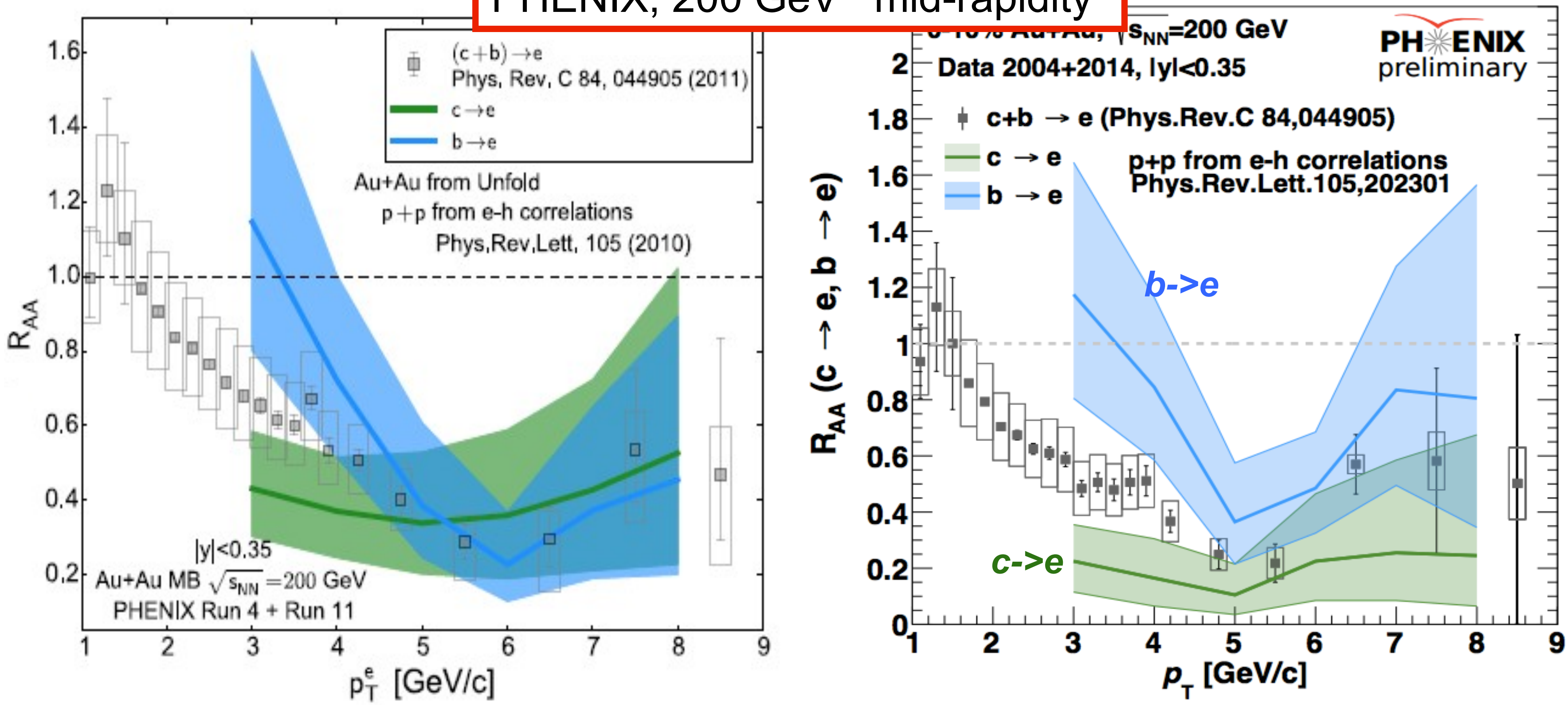

PHENIX, PRC 93 (2016) 034904

- $R_{AA}(e_B) < R_{AA}(e_D)$ at 3 – 5 GeV/c in central Au+Au 200 GeV collisions

mass hierarchy of parton energy loss

Bottom Jet Suppression at LHC

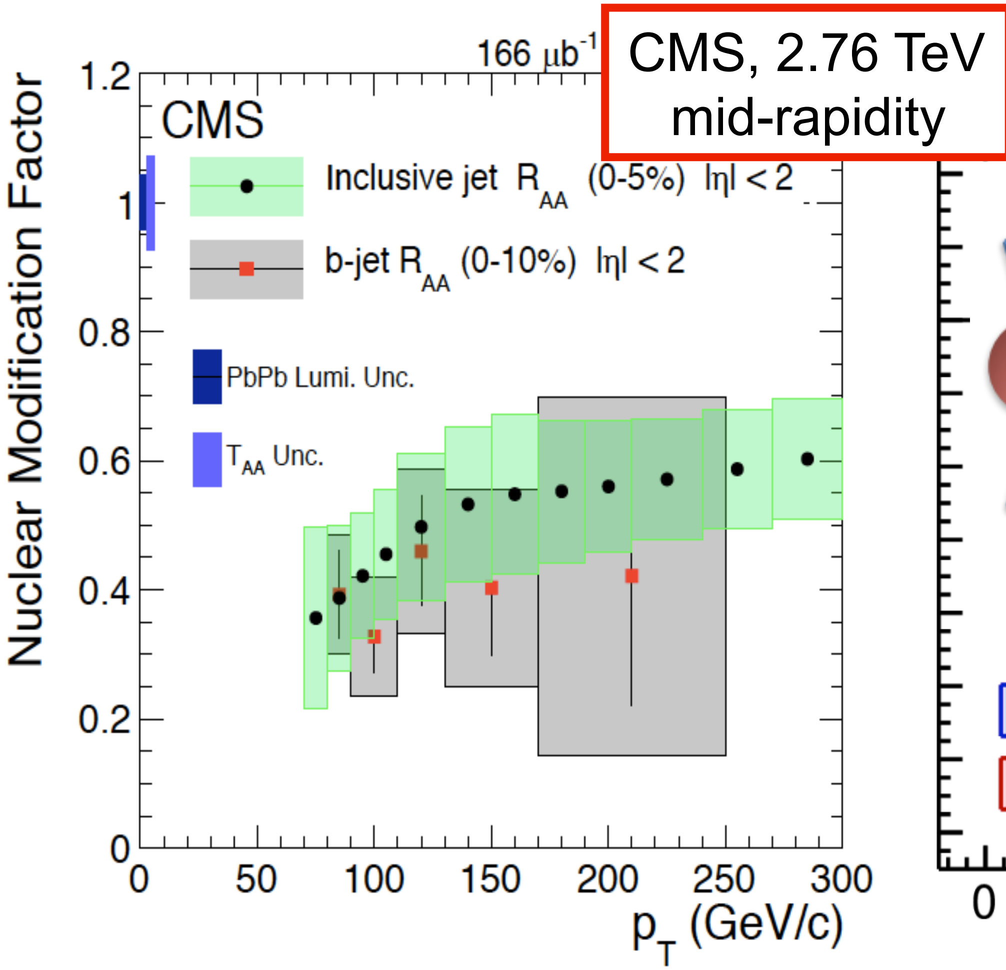

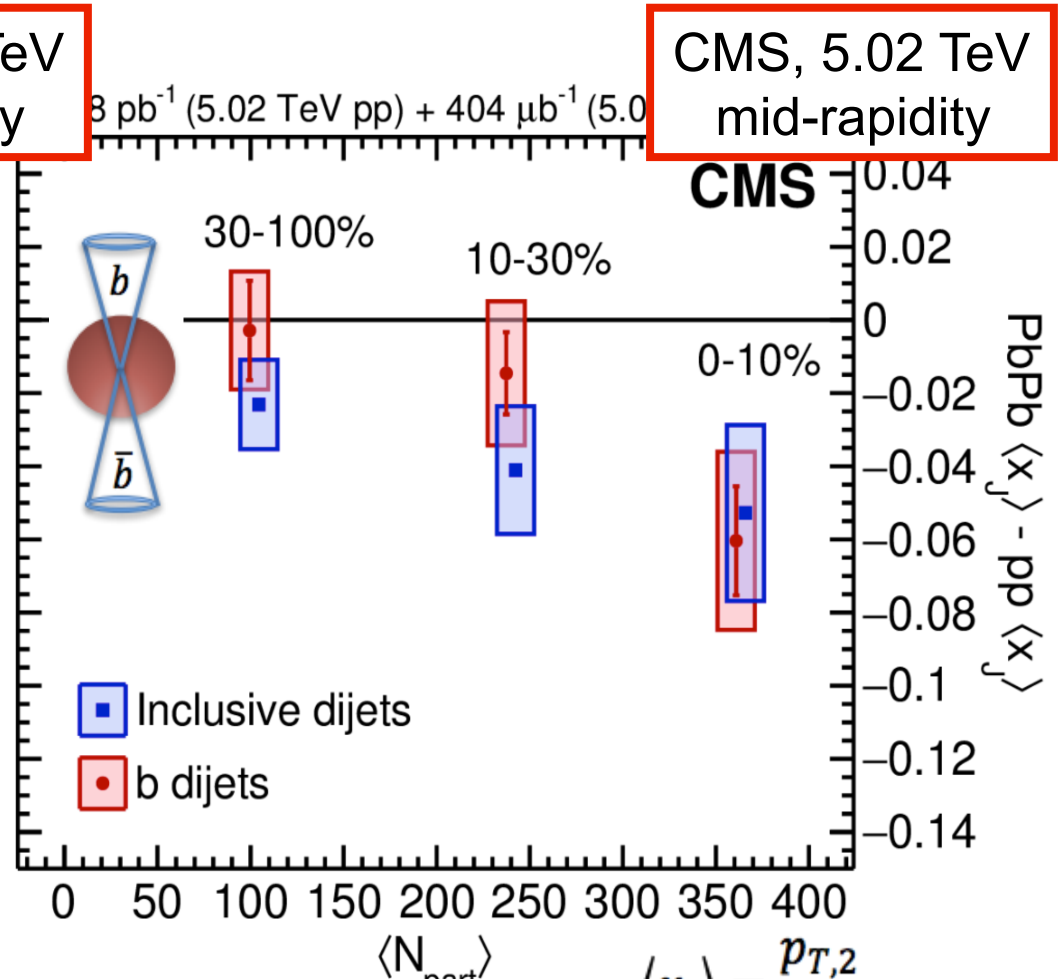

$$\langle x_J \rangle = \frac{p_{T,2}}{p_{T,1}}$$

CMS, PRL 113 (2014) 132301; JHEP 03 (2018) 181

- R_{AA} of inclusive b-jets at p_T>80 GeV/c comparable to that of light jets
- b-dijet $<x_J>$ no significant difference between light and heavy jets vs. centrality

B-meson and non-prompt J/ψ at high p_T

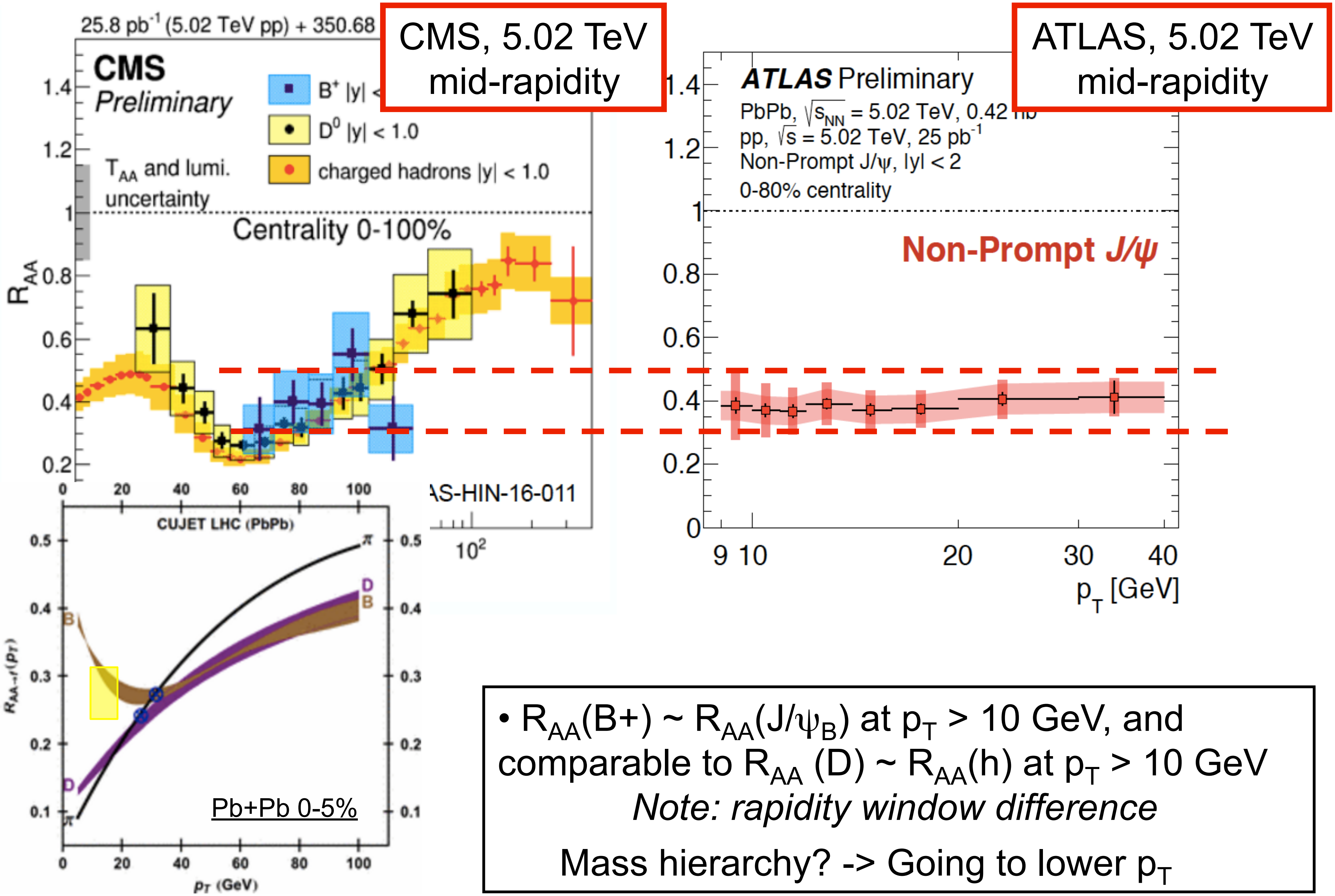

- R_{AA}(B+) ~ R_{AA}(J/ψ_B) at p_T > 10 GeV, and comparable to R_{AA} (D) ~ R_{AA}(h) at p_T > 10 GeV

Note: rapidity window difference

Mass hierarchy? -> Going to lower p_T

Heavy Quark Diffusion Coefficient in QGP

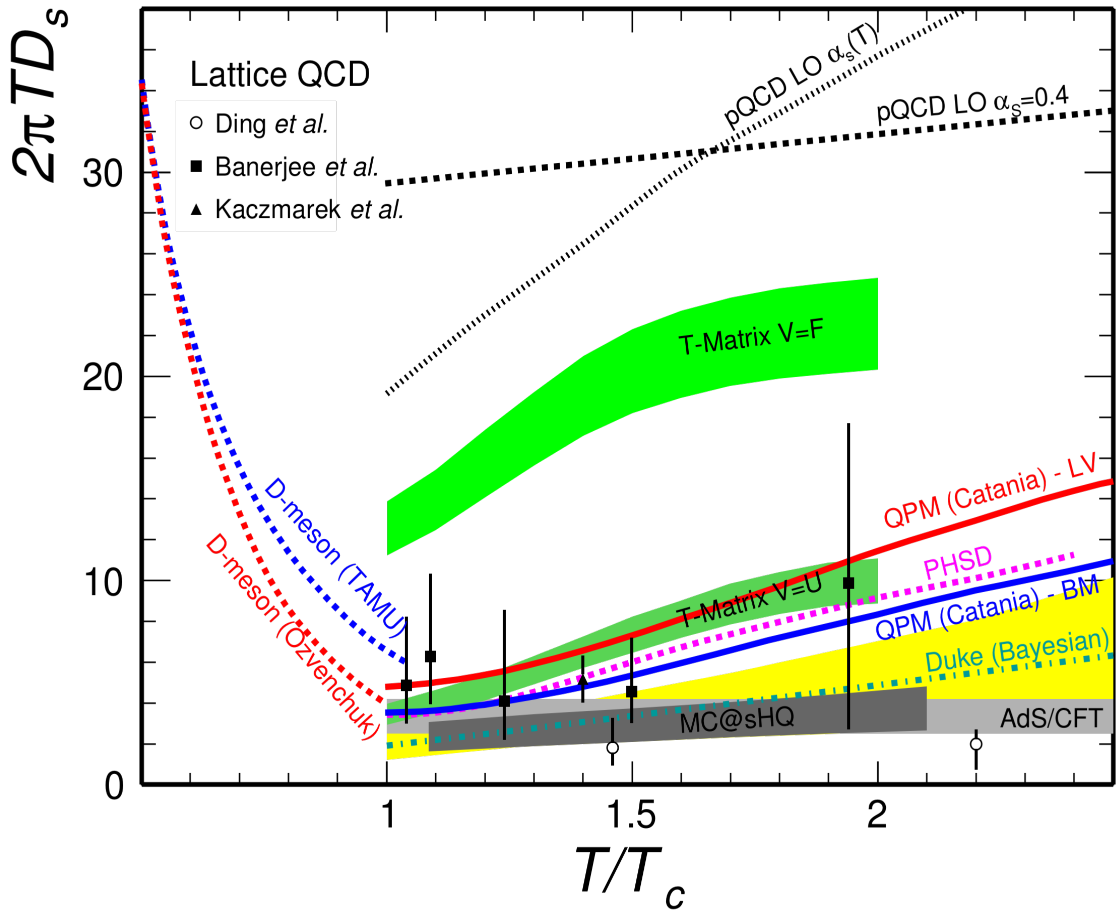

	Temperature (K)	D_s (cm^2/s)
Oxygen (g) in air (g)	298	0.176
Air in water (l)	298	2.00×10^{-5}
Hydrogen in iron (s)	283	1.66×10^{-9}
HQ in QGP	$(1.8\text{-}3.6) \times 10^{12}$	$(100\text{-}600) \times 10^{-5}$

Uniqueness at RHIC

Uniqueness at RHIC

- dominated by pair creation, clean interpretation for experimental results

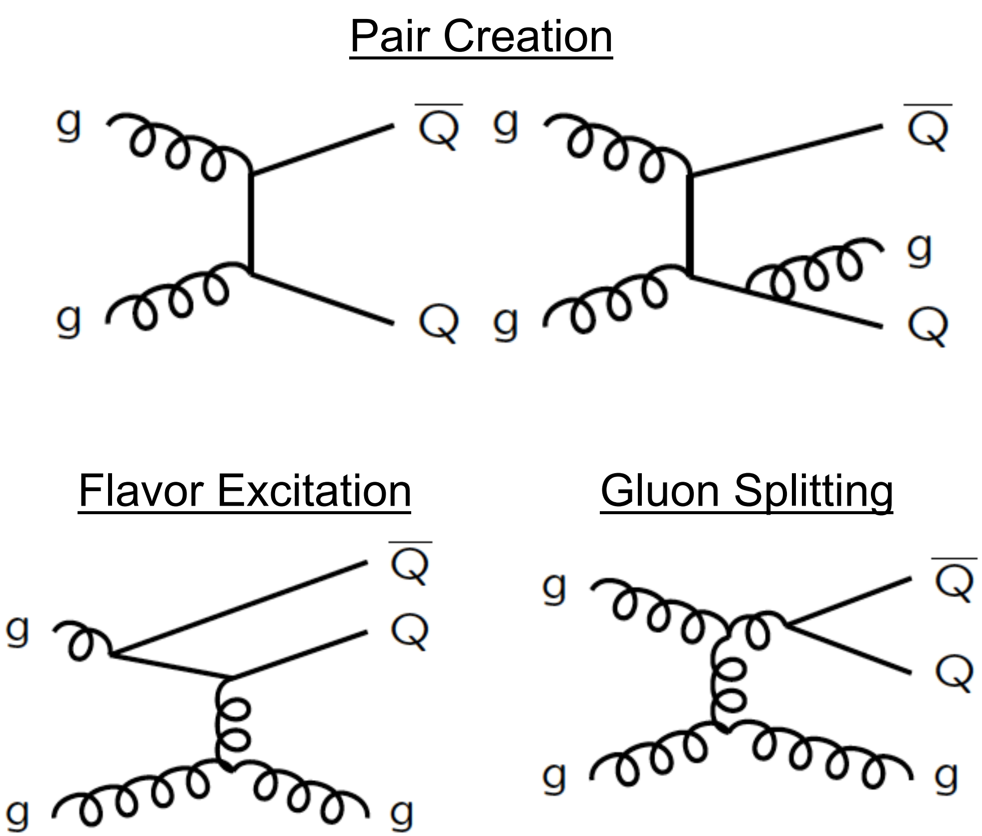

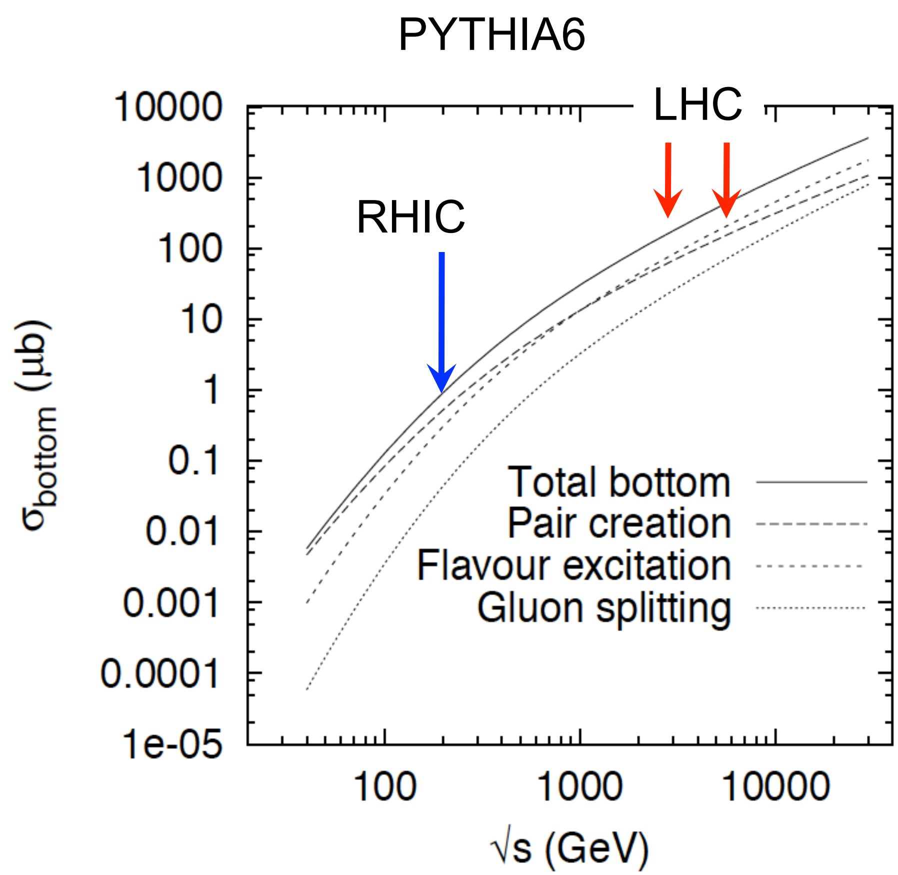

T. Sjostrand, EPJC17 (2000) 137

Bottom Suppression at Low p_T at LHC

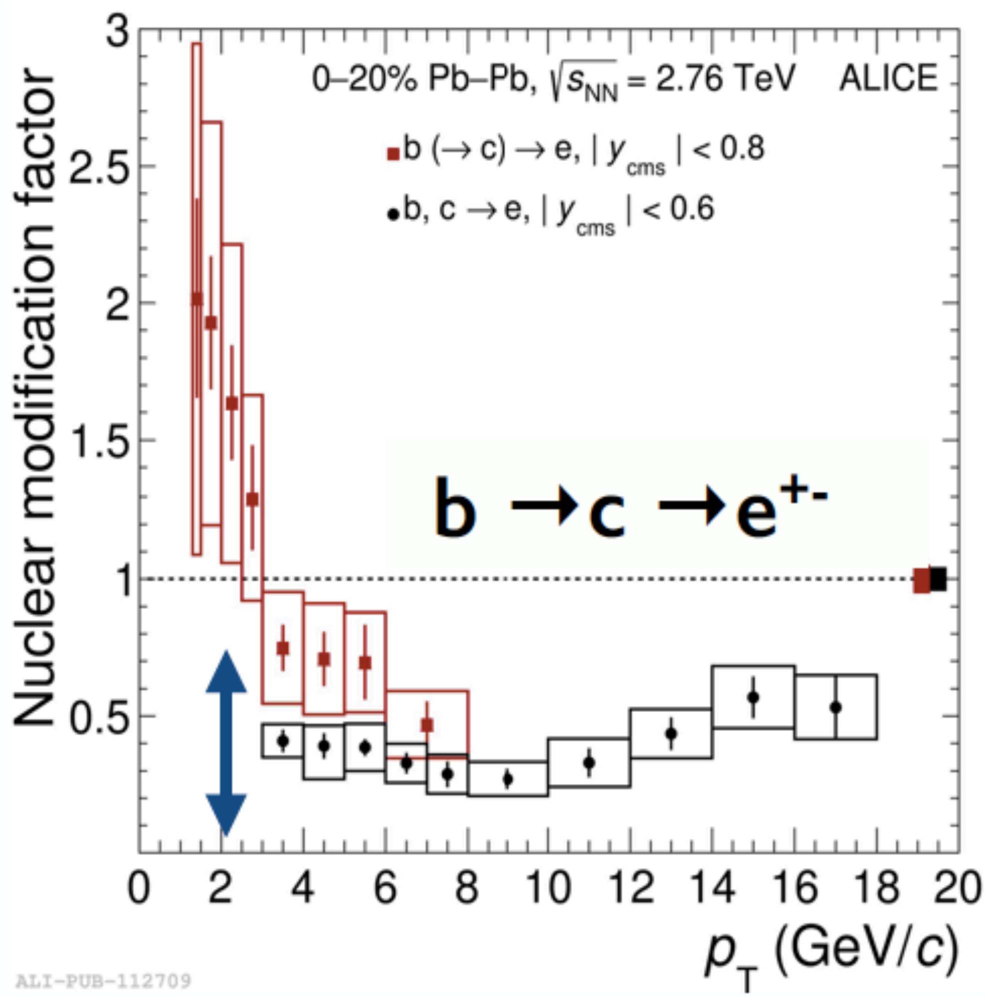

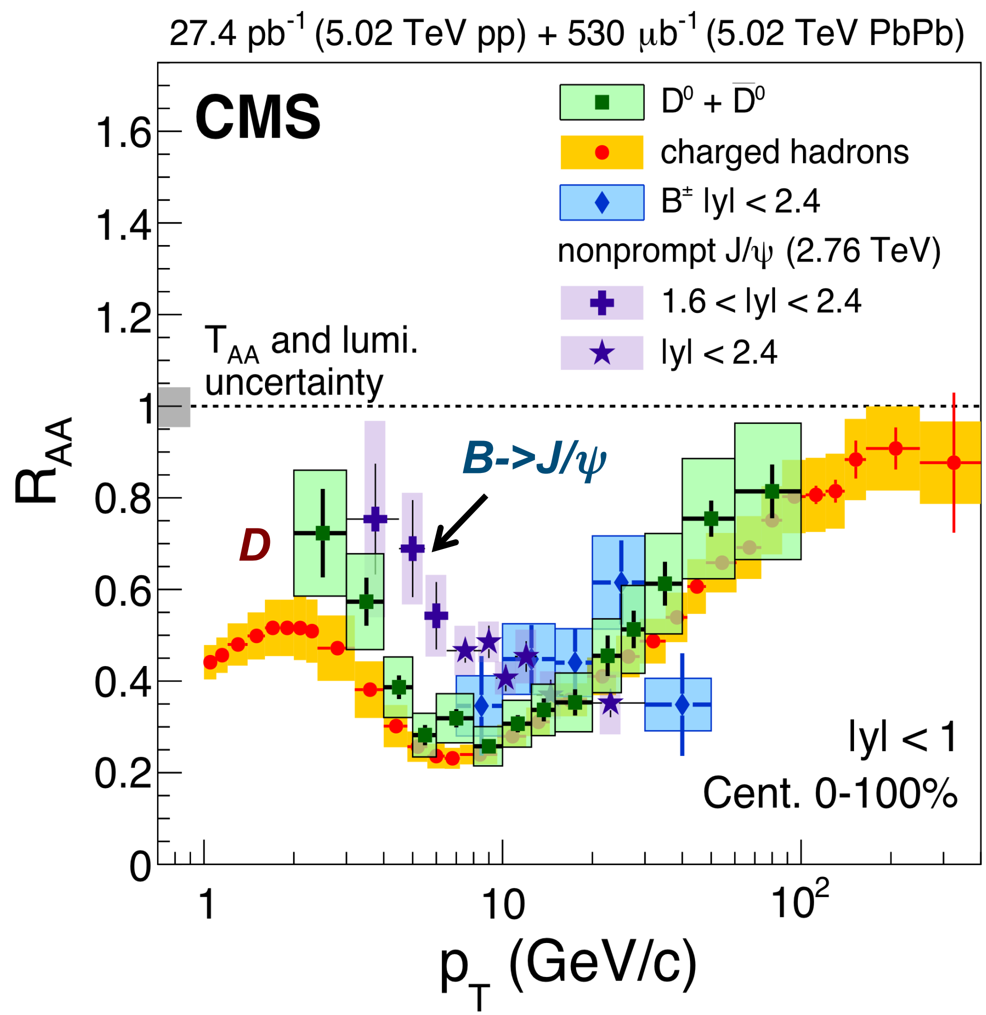

ALICE, JHEP 07 (2017) 052
CMS, arXiv: 1708.04962

- $R_{AA}(e_B) > R_{AA}(e_{C+B})$ and $R_{AA}(J/\psi_B) > R_{AA}(D)$

Evidence of suppression mass hierarchy at low p_T

- consistent with pQCD calculations

D^0 R_{AA} and v_2 Compared to Models at LHC

ALICE 5.02 TeV

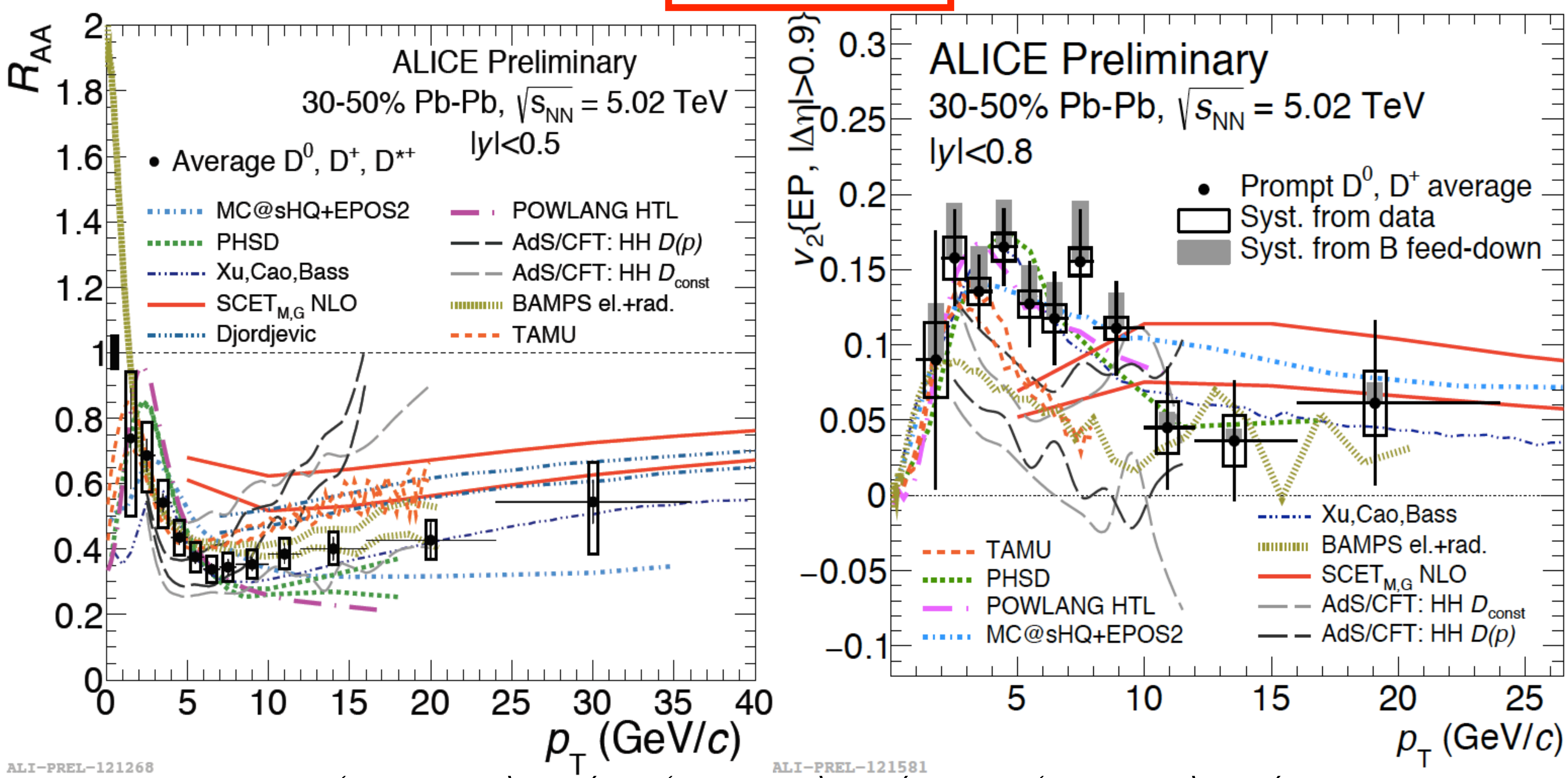

- Charm mesons at LHC show
  significant suppression at high p_T, $R_{AA}(D) \sim R_{AA}(h)$
  significant flow at low-intermediate p_T, $v_2(D) \sim v_2(h)$ vs. m_T-m_0
- Data precision good enough to constrain models

Go Heavier - Open Bottom Production

Open bottom production over a wide range of momentum

Mass/Flavor dependence of parton energy loss

Cleanest probe to quantify medium transport properties – e.g. D_{HQ}

Total bottom yield for precision interpretation of Upsilon suppression

Das et al., PRC 90 (2014) 044901

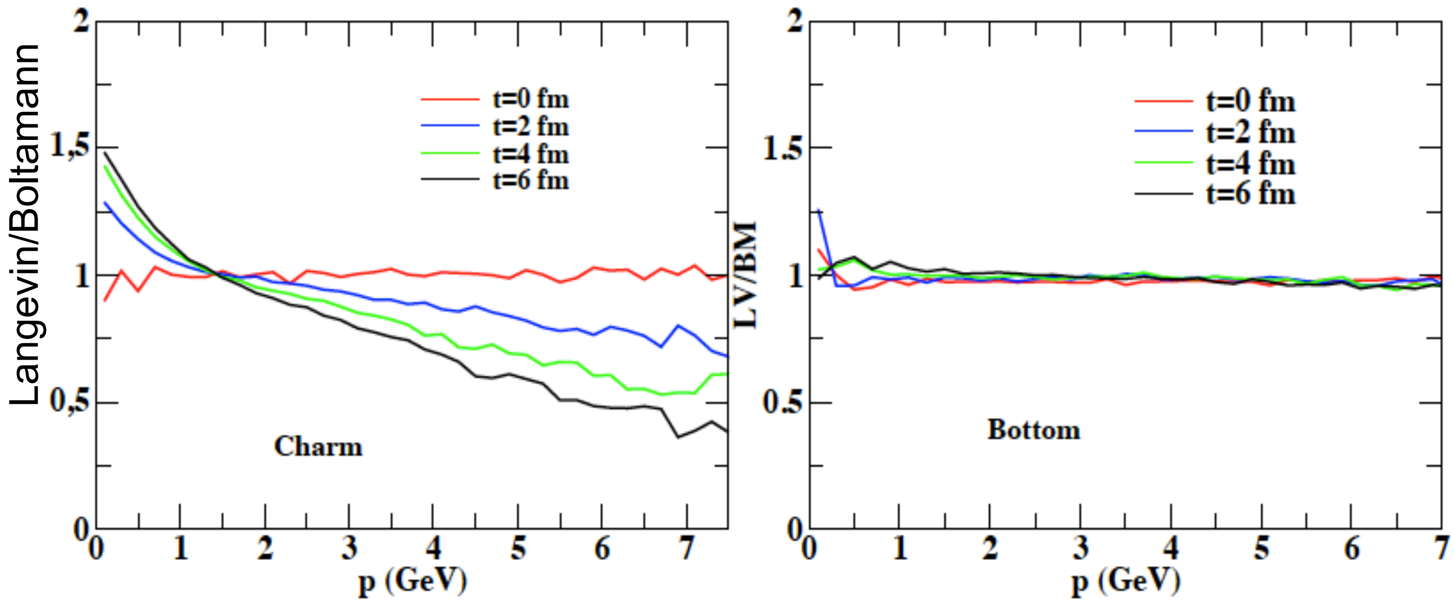

Is charm heavy enough?   Sizable correction to the Langevin approach for charm - may limit the precision in determining D_{HQ}